# Discovery of 4-Amino-*N*-[(1*S*)-1-(4-chlorophenyl)-3-hydroxypropyl]-1-(7*H*-pyrrolo[2,3-*d*]pyrimidin-4-yl)piperidine-4-carboxamide (AZD5363), an Orally Bioavailable, Potent Inhibitor of Akt Kinases

Matt Addie, Peter Ballard, David Buttar, Claire Crafter, Gordon Currie, Barry R. Davies, Judit Debreczeni, Hannah Dry, Philippa Dudley, Ryan Greenwood, Paul D. Johnson, Jason G. Kettle,* Clare Lane, Gillian Lamont, Andrew Leach, Richard W. A. Luke, Jeff Morris, Donald Ogilvie,[†] Ken Page, Martin Pass, Stuart Pearson, and Linette Ruston

Oncology iMed, AstraZeneca, Alderley Park, Macclesfield SK10 4TG, United Kingdom

S *Supporting Information*
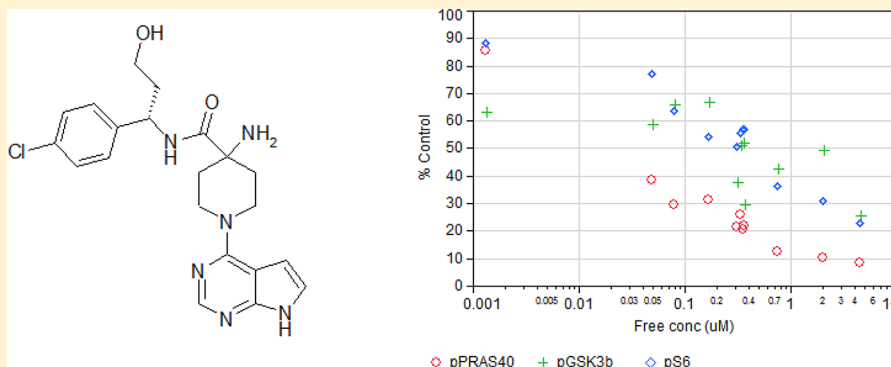
ABSTRACT: Wide-ranging exploration of analogues of an ATP-competitive pyrrolopyrimidine inhibitor of Akt led to the discovery of clinical candidate AZD5363, which showed increased potency, reduced hERG affinity, and higher selectivity against the closely related AGC kinase ROCK. This compound demonstrated good preclinical drug metabolism and pharmacokinetics (DMPK) properties and, after oral dosing, showed pharmacodynamic knockdown of phosphorylation of Akt and downstream biomarkers in vivo, and inhibition of tumor growth in a breast cancer xenograft model.

■ INTRODUCTION

Akt (also known as protein kinase B or PKB) is a serine threonine kinase that acts as a key node in the phosphoinositide 3-kinase (PI3K)−Akt signaling pathway. This axis is one of the most frequently deregulated signaling pathways in human cancers and has been shown to mediate resistance to a range of cytotoxic, antihormonal, and targeted therapies. The pathway plays a critical role in cell growth, proliferation, motility, and survival[1] through modulation of a large number of downstream substrates[2] and is activated by several mechanisms in different cancer types, including somatic mutation, deletion, and amplification of genes encoding key components. Co-localization of Akt with 3-phosphoinositide-dependent protein kinase 1 (PDK1) at the plasma membrane allows the phosphorylation of threonine 308 (Thr308), located in the Akt activation loop. This phosphorylation event is necessary and sufficient for Akt activation.[3] Further phosphorylation of Akt on serine 473 (Ser473), located in the C-terminal hydrophobic motif by the mammalian target of rapamycin (mTOR) complex 2,[4] allows for maximal activation of Akt enzymes. There are three mammalian isoforms of Akt (Akt1, Akt2, and Akt3) that are broadly expressed in most normal tissues and are also expressed in most tumor types to varying degrees. The three enzymes have a similar organizational structure: an N-terminal pleckstrin homology (PH) domain, a central serine/threonine catalytic domain, and a short regulatory region at the C-terminus, also called the hydrophobic motif.[5] A unique feature of the Akt isoforms is the C-terminal extension, which folds back over the ATP site to position two aromatic residues into a hydrophobic groove present in the N-lobe. This results in the occlusion of the solvent channel present in the hinge region of most other kinases.

Due to the strong rationale for targeting Akt in cancer, much effort has been made to identify Akt inhibitors with acceptable pharmaceutical properties, particularly for oral dosing. The most common approaches described to date have been through the development of compounds that are either ATP-competitive or that prevent the formation of the active enzyme.[6] Despite the significant efforts invested in the generation of inhibitors of components of this pathway, it remains unclear whether ATP-competitive or noncompetitive inhibitors

will be most beneficial for the treatment of cancer. A number of Akt inhibitors are currently being tested in clinical trials, including allosteric inhibitors of inactive Akt, such as **1** (MK-2206),[7] and ATP-competitive inhibitors of active enzyme, such as **2** (GDC-0068)[8] (Figure 1) and GSK-2141795.[9] Here we
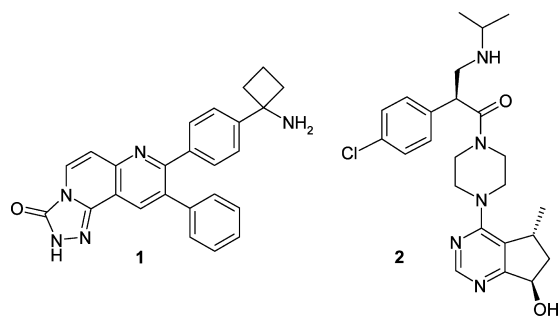
Figure 1. Allosteric inhibitor of inactive Akt, MK-2206 (**1**), and an example of an inhibitor of active Akt, GDC-0068 (**2**).

describe some aspects of the work leading to the discovery of an ATP-competitive Akt inhibitor, 4-amino-*N*-[(1*S*)-1-(4-chlorophenyl)-3-hydroxypropyl]-1-(7*H*-pyrrolo[2,3-*d*]pyrimidin-4-yl)piperidine-4-carboxamide (AZD5363), **64**.

■ RESULTS AND DISCUSSION

Benzylamide **3** has previously been reported as an orally bioavailable inhibitor of Akt. This compound was originally identified as a suitable starting point for further optimization as a result of our prior collaboration with Astex Therapeutics Ltd. and their collaboration with the Institute of Cancer Research.[10] This lead arose from a fragment-based screening campaign from which several alternative hinge binding groups were found, which were then elaborated into potent Akt inhibitors; a selection of the chemotypes explored are highlighted in Figure 2.[11]

Common features of these inhibitors include a small hinge-binding heteroaromatic ring presenting a donor–acceptor motif to Glu228 and Ala230, a phenyl or piperidine spacing group, a primary or secondary amino functionality that can form a H-bonding interaction with the acid hole formed by Glu234 and Glu278, and a lipophilic aromatic group that is positioned in a hydrophobic pocket under the P-loop of the ATP-binding site. This pharmacophore for ATP-competitive inhibition of Akt matches has subsequently been reported by a number of other groups.[12] Following thorough evaluation of the various lead series, we elected to work on the benzylamide series as exemplified by compound **3**, as its efficacy and tolerability were favorable. Key data for **3** are listed in Table 1. Compound **3** is a

Table 1. Profiling of Early Lead Akt Inhibitor 3

| parameter	value
enzyme potency IC_{50} (nM) [Akt1, Akt2, Akt3]	13, 66, 57
cell $IC_{50}{}^{a}$ (nM)	328
ROCK2 IC_{50} (nM), *n*-fold-selectivity	66, 5
log *D*, pH 7.4	2.9
plasma protein binding, % free [mouse, rat, dog, human]	14, 14, 11, 22
solubility, pH 7.4 (μM)	150
hERG IC_{50} (nM)	5235
hepatocyte Cl_{int} (μL·min^{-1}·(10^6 cells)$^{-1}$) [mouse, rat, dog, human]	10, 19, 6, 15
Cl (mL·min^{-1}·kg^{-1}) [mouse, rat, dog]	42, 48, 2
Vd_{ss} [mouse, rat, dog]	2.8, 3.1, 0.6
$t_{1/2}$ (h) [mouse, rat, dog]	0.8, 2.3, 3.0
F (%) [mouse, rat, dog]	88, 56, 70

^{a}Inhibition of pGSK3β by Akt.

reasonably potent enzyme inhibitor of all three Akt isoforms and is a moderately potent inhibitor of phosphorylation of glycogen synthase kinase 3β (GSK3β) by Akt in human MDAMB468 cells. Following oral dosing, **3** had also demonstrated
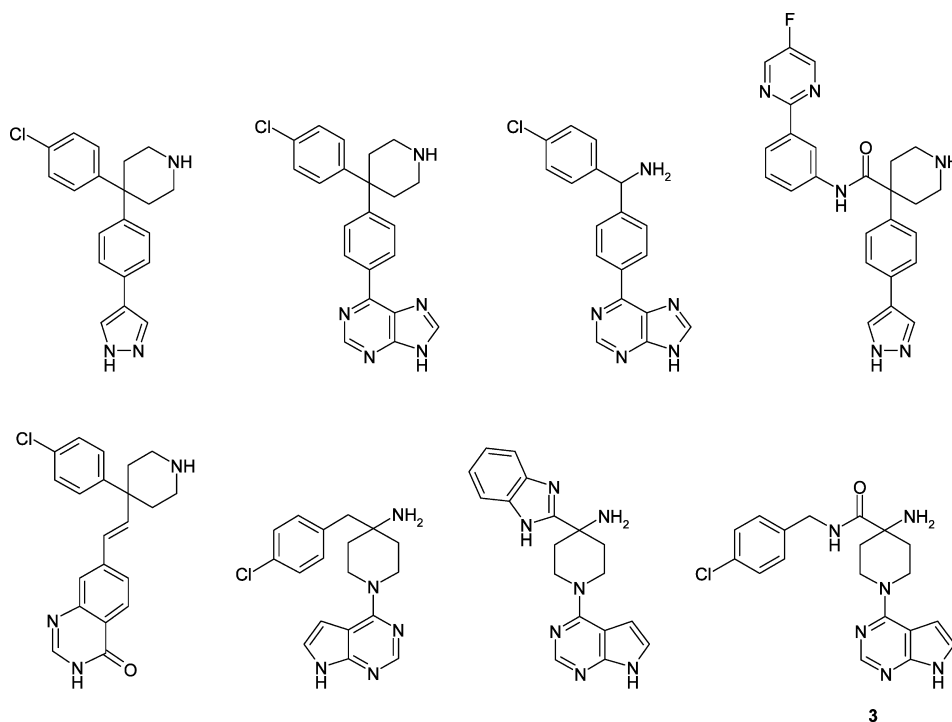
Figure 2. Inhibitors of Akt arising from collaboration with Astex Therapeutics Ltd. and the Institute of Cancer Research.[10,11]

Scheme 1. General Synthesis of Akt Inhibitors 7[a]
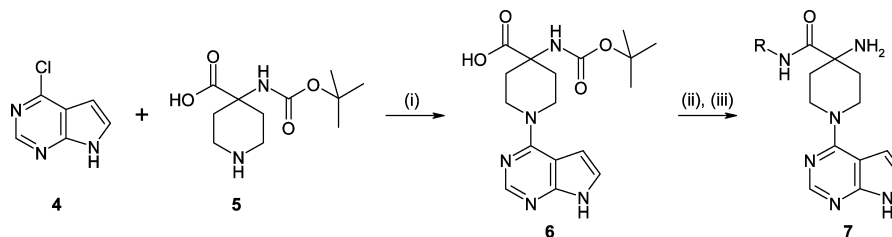
[a]Reagents and conditions: (i) NaHCO$_3$, CH$_3$CN/H$_2$O, reflux 24 h; (ii) N-(3-dimethylaminopropyl)-3-ethylcarbodiimide, HBT, DMF, 16 h; (iii) 4 M HCl in dioxane, RT, 16 h.

Scheme 2. Synthesis of Representative Substituted Benzylamines Used in the Elaboration of Akt Inhibitors 45, 61, and 63[a]
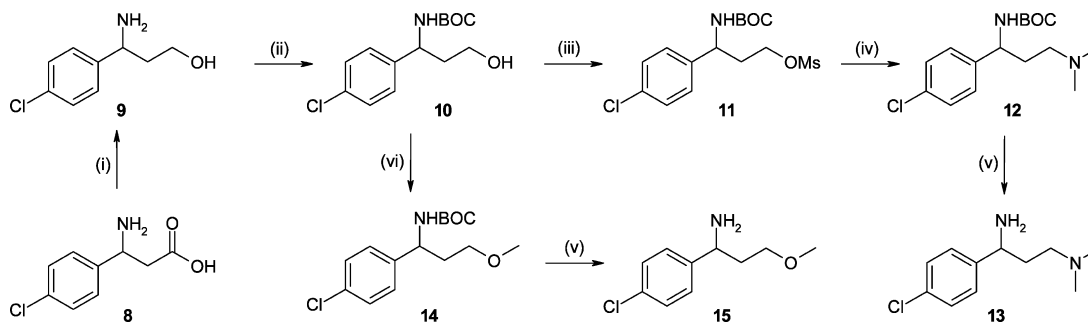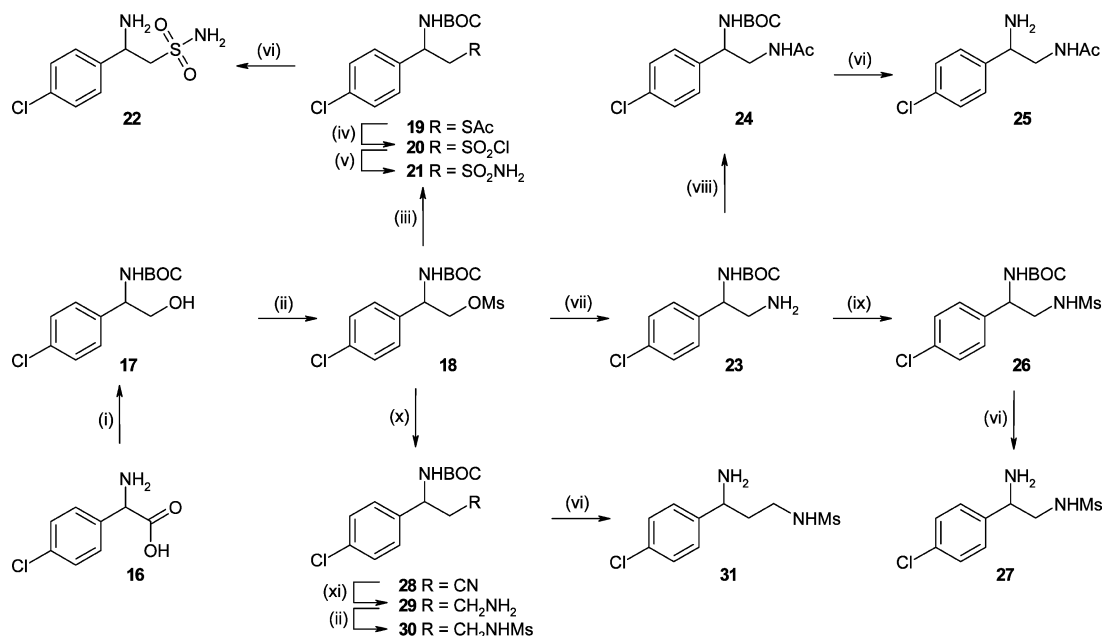

[a]Reagents and conditions: (i) BH$_3$·THF, RT, 5 h; (ii) di-tert-butyl dicarbonate, DCM, RT, 2 h; (iii) MsCl, Et$_3$N, DCM, RT, 2 h; (iv) Me$_2$NH, TBAI, THF, 150 °C, 0.5 h; (v) 4 M HCl, dioxane, DCM, methanol, RT, 4 h; (vi) NaH, MeI, THF, RT, 4 h.

pharmacodynamic inhibition of Akt pathway signaling and demonstrated growth inhibition in a relevant xenograft model.[10] However, enzyme selectivity over closely related ROCK2 was judged to be insufficient at just 5-fold based on enzyme activity. ROCK2 is another member of the AGC kinases and is involved in regulation of vascular tone and thus control of blood pressure. There is high homology within the AGC kinase family, with Akt1 and ROCK2 sharing 40% sequence identify (53% similarity) in the kinase domain; this increases to 86% sequence identity (100% similarity) when the 15 residues within 3 Å of ATP are considered. A selective ROCK inhibitor has been shown to significantly decrease blood pressure and cause increased heart rate and cardiac contractility in a canine in vivo cardiovascular model.[13] Our extensive structure–activity relationship (SAR) studies exploring the series had revealed that achieving selectivity over ROCK while retaining Akt potency was challenging. At the same time, we aspired to resolve the issue of activity at the hERG ion channel, given that compound 3, with an IC$_{50}$ of 5 μM for inhibition, may present issues further in development. Activity against the hERG ion channel is implicated in the development of Torsades de Pointes and sudden cardiac death. Despite these issues, 3 demonstrated good pharmacokinetics across three species, showing reasonable absorption and low to moderate clearance. In vitro hepatic clearance values were also low, including importantly in human cells. It is noteworthy that this good drug metabolism and pharmacokinetics (DMPK) profile is observed in the presence of the required primary amino pharmacophore. We speculate that the combination of close proximity to the electron-withdrawing amido group, coupled with high steric hindrance at this tertiary center, mitigates against the clearance and absorption issues one might otherwise anticipate.

Chemistry. Inhibitors of Akt described in this work were generally assembled in a short sequence from readily available starting materials (Scheme 1). Piperidine 5 and chloroheterocycle 4 were condensed to give the key carboxylic acid building block 6, which was subsequently coupled with a variety of primary amines to give the requisite amide group. Acid-promoted deprotection of the primary amine functionality revealed Akt inhibitors 7. The amines used in this coupling were often commercially available; however, representative examples of the synthesis of more complex coupling partners is outlined in Schemes 2 and 3.

Amino acid 8 was reduced to amino alcohol 9, which was coupled to building block 6 to give, after deprotection, inhibitor 61. Amino alcohol 9 also served as a useful precursor to bis-amine 13 and ether 14, used in the synthesis of Akt inhibitors 45 and 63, respectively. The alcohol was converted to mesylate 11, which in turn gave bis-amine 13 by displacement with dimethylamine and subsequent deprotection of the benzylamine moiety. Alternatively, simple alkylation of 10 with methyl iodide gave ether 15 after removal of the protecting group. Similarly, amino acid 16 was used as a starting material for a range of differently substituted benzylamines. Reduction of the acid and in situ protection of the amino group gave alcohol 17, with subsequent mesylate ester 18 proving a versatile intermediate for introduction of a range of polar substituents. Thioester formation and N-chlorosuccinimide-promoted oxidation give sulfonyl chloride 20. Quenching with ammonia and amine deprotection yielded β-aminosulfonamide 22, used in the synthesis of inhibitor 56. Primary amine 23 was also synthesized from mesylate 18 through azide displacement and reduction. This amine was capped with an acyl group to give 25 or with a mesyl group to give 27, and these ultimately yielded Akt inhibitors 55 and 58, respectively. Mesylate 18 was also used to access higher alkyl homologues such as 31, used to deliver inhibitor 59. Displacement with cyanide gave nitrile 28, which was reduced to primary amine 29. As before, capping

Scheme 3. Synthesis of Representative Substituted Benzylamines Used in the Elaboration of Akt Inhibitors 55, 56, 58, and 59[a]

[a]Reagents and conditions: (i) NaBH$_4$, I$_2$, THF, reflux, 12 h, and then di-*tert*-butyl dicarbonate, Et$_3$N, RT, 2 h; (ii) MsCl, DIPEA, DCM, RT, 2−18 h; (iii) KSAc, DMF, 50 °C, 1 h; (iv) NCS, 2 M HCl, CH$_3$CN, 10 °C, 0.3 h; (v) NH$_3$, CH$_3$CN, RT, 16 h; (vi) TFA, RT, 0.3 h; (vii) NaN$_3$, DMF, 80 °C, 1 h, and then H$_2$, 10% Pd/C, ethanol, RT, 1 h; (viii) Ac$_2$O, DIPEA, THF, RT, 2 h; (ix) MsCl, DIPEA, THF, RT, 2 h; (x) NaCN, DMF, 80 °C, 3 h; (xi) LiAlH$_4$, THF, RT, 2 h.
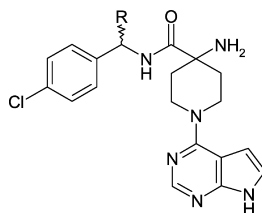
with a mesyl group and deprotection yielded amine **31**. Further details of all the routes used to make the compounds described herein can be found in the Supporting Information.

α-Substitution with Alkyl Groups. A crystal structure of **3** bound to Akt2 was available to AstraZeneca from our collaboration[10] (PDB code 2X39), which showed that the pyrrolopyrimidine of **3** formed hydrogen bonds to the hinge domain, the amino group interacted with an acidic hole, and the *p*-chlorophenyl group entered a pocket under the P-loop. SAR around this lead has been reported, although no further improvements in potency were found in the analogues tested.[10] Indeed, our own extensive medicinal chemistry exploration of this lead also indicated many different modifications ultimately proved unproductive in achieving the desired combination of properties, including changes to the hinge binding group, amide functionality, and any changes to the nature and position of the primary amine. We were intrigued, however, by the potential to substitute on the α-carbon of the benzyl group, since inspection of the available crystal structure suggested space to accommodate such a change. No obvious interactions would result from this, however, so it was unclear what effect this would have on potency or other key properties. Initially the racemic α-methylated compound **32** was synthesized, and despite showing broadly similar enzyme potency to **3**, a modest improvement in cell activity was observed, in addition to slightly better selectivity. To understand whether one isomer was more responsible than the other for this profile, both individual enantiomers were synthesized. The *S*-enantiomer **34** proved significantly more active than the *R*-enantiomer **33**, and despite absolute ROCK activity also being greater in **33**, the improvements in Akt enzyme potency meant the selectivity ratio was also improved (Table 2). No significant movement in hERG inhibition was observed for this small change, however. It was hypothesized that the introduction of the α-methyl chiral center

introduced a ligand conformational preference with respect to the P-loop aryl group and consequently that the selectivity differences observed could potentially arise from differences in the nature of the P-loop hydrophobic pocket between Akt1 and ROCK2. If this hypothesis was correct, different selectivity profiles might be achievable, enhancing Akt1 potency and reducing ROCK2 potency through the development of ligands that might exploit this proposed difference.

Additional α-alkyl analogues were synthesized to explore the effect of further substitution, and for synthetic convenience the initial follow-up studies were performed with racemic samples. Small lipophilic substituents such as ethyl **35** and cyclopropyl **36** showed similar potency to methyl, and hERG activity was also unchanged, although ROCK selectivity was improved, particularly for the latter (Table 2). Larger α-substituents were generally less potent in both enzyme and cell assays. The compound with an α-phenyl group, **37**, led to a significant reduction in cellular potency, as did other compounds with large aromatic substituents such as the benzylic analogue **38** (Table 2). Alkyl substituents larger than methyl generally came with an expected increase in lipophilicity and concomitant reduction in solubility, and this issue was particularly acute for α side chains that contained aromatic rings. For these larger groups, hERG inhibition also appeared to increase in line with log *D*.

Aromatic Ring Substitution. Previous studies had demonstrated that while a range of other pendant phenyl substituents could be tolerated, in the limited compounds studied, a *p*-chloro group offered the best overall balance, particularly with respect to potency.[10] As methyl appeared to be the optimal α-substituent in this initial limited expansion, this group was fixed and variation of the aromatic ring in the benzyl group was revisited in an attempt to explore in particular the effect on hERG potency. Table 3 shows a selection of the aromatic

Table 2. Akt Enzyme and Cell Potency, Selectivity, and hERG Activity for α-Alkyl-Substituted Benzylamide Analogues

		IC$_{50}$ (nM)							
	R	Akt1[a]	Akt2[a]	Akt3[a]	cell[b]	ROCK2[c]	hERG[d]	log D	solubility[e] (μM)
3	H	13	66	57	328	66 [5]	5235	2.9	150
32	Me	8	40	30	197	101 [13]	7200	2.7	180
33	R-Me	276	836	523	4594	1396 [5]	9092	3.3	77
34	S-Me	4	20	16	134	55 [15]	6747	2.7	110
35	Et	7	23	15	144	126 [19]	6495	3.5	13
36	c-Pr	5	30	24	208	261 [52]	2600	3.4	31
37	Ph	41	210	270	1620	576 [14]	1600	4.1	<1
38	Bn	31	190	150	1650	586 [19]	3500	4.1	<1

[a]All IC$_{50}$ data are the mean of at least n = 2 independent measurements. Each has a standard error of measurement (SEM) ±0.2 log unit. [b]Inhibition of phosphorylation of GSK3β mediated by Akt in MDAMB468 cells. [c]Value in brackets indicates enzyme selectivity ratio to Akt1. [d]CHO cells, IonWorks assay. [e]Thermodynamic solubility in 0.1 M phosphate buffer at pH 7.4 (25 °C).

Table 3. Akt Enzyme and Cell Potency, Selectivity, and hERG Activity for Selected Aryl-Substituted Benzylamide Analogues
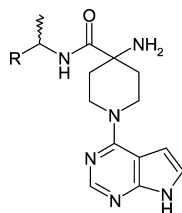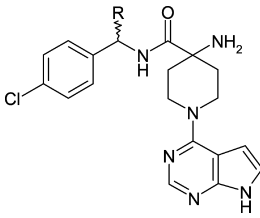

		IC$_{50}$ (nM)							
	R	Akt1[a]	Akt2[a]	Akt3[a]	Cell[b]	ROCK2[c]	hERG[d]	log D	solubility[e] (μM)
39	phenyl	149	709	582	6710	132 [1]	>33300	2.2	98
40	4-F-phenyl	9	344	176	1776	135 [15]	26957	2.4	96
41	3-pyridyl	1313	8111	4260	>30132	1297 [1]	>33300	1.2	> 2600
42	2-pyridyl	2753	16498	8065	>3250	3149 [1]	>33300	1.3	> 2400
43	4-(methylsulfonyl)phenyl	183	805	756	5165	1144 [6]	>33300	1.0	230
44	3,4-dimethoxyphenyl	1192	8578	2893	>3250	1072 [1]	>100000	1.8	> 740

[a]All IC$_{50}$ data are the mean of at least n = 2 independent measurements. Each has a SEM ±0.2 log unit. [b]Inhibition of phosphorylation of GSK3β mediated by Akt in MDAMB468 cells. [c]Values in brackets indicate enzyme selectivity ratio to Akt1. [d]CHO cells, IonWorks assay. [e]Thermodynamic solubility in 0.1 M phosphate buffer at pH 7.4 (25 °C).

substitutions examined, all in a racemic α-methyl series to aid synthetic tractability. Removal of the chloro group to give unsubstituted compound **39** resulted in a reduction in potency, at both the enzyme and cellular level, consistent with earlier observations. Introduction of a *p*-fluoro group as in compound **40** recovered some of this potency, but not to the level seen with chloro analogue **32**. In both these examples however,

absolute hERG affinity was lowered, broadly consistent with lowered lipophilicity, but this did not result in improvements to solubility. Heterocycles in this region were also poorly tolerated, with both 2- and 3-pyridyl analogues **41** and **42** showing no cellular activity at the top concentration tested. Despite significant improvements in both hERG activity and solubility for this change, selectivity at the enzyme level versus ROCK was also

Table 4. Akt Enzyme and Cell Potency, Selectivity, and hERG Activity for α-Substituted Benzylamide Analogues Carrying a Basic Side Chain

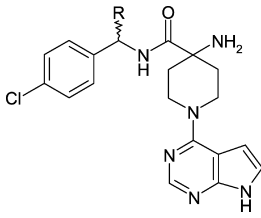|		IC$_{50}$ (nM)							
	R	Akt1[a]	Akt2[a]	Akt3[a]	Cell[b]	ROCK2[c]	hERG[d]	log D	solubility[e] (μM)
45		2	14	7	96	31 [16]	>100000		
46		3	15	4	126	71 [25]	>100000	1.4	> 1700
47		4	96	36	209	104 [29]	>100000	1.3	> 1500
48		5	42	15	156	134 [25]	74807	2.7	1400
49		5	30	10	81	112 [24]	>33300		
50	S-	3			110	34 [12]	>33300		2320
51	S-	4	31	18	43	39 [10]	21030		>2470
52	S-	4	13	6	78	34 [10]	29367	2.4	>2090

[a]All IC$_{50}$ data are the mean of at least n = 2 independent measurements. Each has a SEM ±0.2 log unit. [b]Inhibition of phosphorylation of GSK3β mediated by Akt in MDAMB468 cells. [c]Values in bracketss indicate enzyme selectivity ratio to Akt1. [d]CHO cells, IonWorks assay. [e]Thermodynamic solubility in 0.1 M phosphate buffer at pH 7.4 (25 °C).

severely compromised. A range of other simple substitions were explored as typified by sulfone **43** and dimethoxy analogue **44**. The picture relative to chloro lead **32** was again consistent, with compounds often showing improved hERG margin, but generally weaker Akt cell activity and compromised selectivity profile.

α-Substitution Carrying a Basic Side Chain. Following initial exploration of the vector provided by the benzyl methylene group that led to S-Me analogue **34**, this region was revisited with a broader range of functionalities. The impact of appending basic groups in this region was explored with a focused set of targets, since although the modest solubility of lead **3** does not compromise its pharmacokinetic profile, further improvements might be beneficial. Initial exploration targeted a dimethylamino side chain as in homologues **45** and **46**. Both analogues showed potent enzyme and cellular inhibition, with a three-carbon side chain seemingly offering modest advantage over a two-carbon side chain with respect to ROCK selectivity. In both molecules hERG activity is dramatically reduced. Further exploration of the SAR around the basic group with analogues such as pyrrolidine (**47**), morpholine (**48**), and piperidine (**49**) led to compounds with a very similar overall profile: improved potency and selectivity and lowered hERG

affinity (Table 4). A number of chirally pure S-enantiomers were also synthesized. Compound **50** is the S-enantiomer of racemate **45**, and in this case the profile is largely identical with **50**, showing potent cell activity, high solubility, and good hERG margin, albeit with a lower selectivity over ROCK. Varying the base further, such as with pyrrolidine **51** or piperidine **52**, again led to compounds with a good balance of properties but with lower than ideal ROCK selectivity (Table 4). Single S-isomers **50**−**52** were all tested in a rat DMPK study and all showed clearance at a rate significantly in excess of liver blood flow, and consequently no oral bioavailability (Table 4). A contribution to this from limited absorption cannot be ruled out, however.

α-Substitution Carrying a Neutral Side Chain. Since side chains carrying a basic group had led to high clearance and low oral bioavailability, the exploration of nonbasic polar substituents was initiated. Amides **53** and **54** and reversed amide **55** showed much reduced hERG activity, but cell potency and overall ROCK selectivity was compromised (Table 5). A similar profile was observed with sulfonamides **56** and **57**, one of compromised cell activity and selectivity. Two-carbon side-chain analogue **56** showed slightly greater activity than the three-carbon analogue **57** but worse absolute selectivity, and solubility was poor despite comparable log D to other examples (Table 5).

Table 5. Akt Enzyme and Cell Potency, Selectivity, and hERG Activity for α-Substituted Benzylamide Analogues Carrying a Neutral Side Chain

	R	IC$_{50}$ (nM)						log D	solubility^e (μM)
		Akt1^a	Akt2^a	Akt3^a	Cell^b	ROCK2^c	hERG^d		
53		30	159	105	1126	351 [12]	>100000	2.2	460
54		42	-	-	681	266 [6]	>33300	2.4	400
55		31	-	-	2893	182 [6]	>33300	2.4	> 1200
56		12	-	-	489	37 [3]	>33300	2.2	5
57		6	-	-	874	62 [10]	>33300		
58		16	-	-	995	90 [6]	>33300	2.1	29
59		7	36	30	414	153 [22]	80124	2.2	86
60		7	46	40	302	89 [12]	>100000	2.4	47
61		4	22	15	91	112 [27]	>100000	2.5	21
62		6	24	22	138	76 [12]	57793	2.8	130
63		10	130	100	303	204 [22]	9369	3.0	52
64 AZD5363		3	8	8	89	56 [18]	>100000	2.5	780

^{a}All IC$_{50}$ data are the mean of at least $n = 2$ independent measurements. Each has a SEM ±0.2 log unit. ^{b}Inhibition of phosphorylation of GSK3β mediated by Akt in MDAMB468 cells. ^{c}Values in brackets indicate enzyme selectivity ratio to Akt1. ^{d}CHO cells, IonWorks assay. ^{e}Thermodynamic solubility in 0.1 M phosphate buffer at pH 7.4 (25 °C).

This pattern was reinforced when the sulfonamide was reversed, as in **58** and **59**, where again a two-carbon spacer in compound **59** gave better cell activity, and here improved selectivity, over the shorter one-carbon linker in **58** (Table 5). Both compounds had an acceptable hERG margin, but again, sulfonamides consistently demonstrated only modest solubility. The impact of spacing a hydroxyl substituent at varying distances from the methylene group was explored with homologues **60−62**. As before, a clear preference for a two-carbon spacer emerged, with **61** showing the greatest cell potency, ROCK selectivity and hERG margin (Table 5). One-carbon spacing as in **60** also had much reduced hERG potency but with compromised cell

potency, and three-carbon spacing in **62**, while more potent than **60**, showed measurable hERG inhibition. Methylating **61** to give ether **63** led to an increase in lipophilicity, much increased hERG inhibition, and also compromised cellular potency. Finally, isolation of the more active *S*-enantiomer of **61** gave **64**, subsequently designated AZD5363. This compound showed potent pan-Akt enzyme inhibition (3−8 nM) and cell activity (89 nM), high hERG margin (>100 000),h excellent solubility, and 18-fold selectivity for Akt1 enzyme over ROCK2 (Table 5). The corresponding *R*-enantiomer was synthesized and exhibited markedly lower enzyme and cell potency of 90 nM and 3300 nM respectively, confirming a chiral preference for binding.
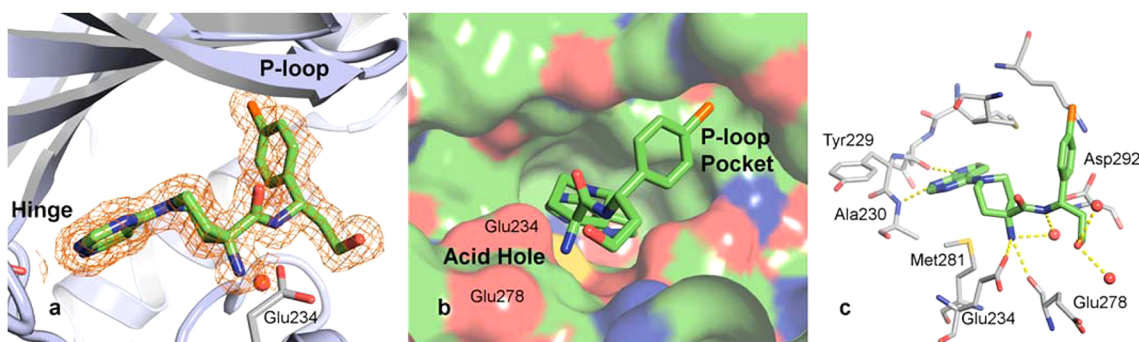
Figure 3. (a) Ligand binding mode of compound **64** in Akt1 determined by X-ray crystallography at 1.49 Å resolution. The $2F_o - F_c$ electron density map is displayed in orange and contoured at 1σ around the inhibitor. Nearby water molecules are represented as red spheres. (b) Molecular surface representation of the Akt1 binding pocket, looking toward the kinase hinge region. (c) Hydrogen-bond network formed by **64** and Akt1 residues within 3 Å of the inhibitor.

X-ray Crystallographic Studies. A crystal structure of **64** bound to Akt1 (PDB code 4GV1) was obtained (Figure 3). This revealed key interactions and features that may contribute to the high Akt affinity of this compound. The protein is in the active form with the C-terminal tail folding back over the N-terminal lobe to position Phe469 and Phe472 in the hydrophobic pocket essential for regulatory control of Akt1. The pyrrolopyrimidine ring forms two hydrogen bonds to the kinase hinge through residues Ala230 and Glu228. Interestingly, the central piperidine ring adopts an axial conformation with respect to both the pyrrolopyrimidine hinge group and the P-loop aryl group. This axial over equatorial preference is influenced by the ortho-sp^2 nitrogen in the pyrrolopyrimidine core, and adoption of this conformation positions the basic amino group in the acidic hole formed by Glu234 and Glu278, and the *p*-chlorophenyl group in a hydrophobic pocket under the P-loop formed by the side chains of Lys179, Leu181, and Val164 and backbone atoms of Lys158 and Gly162. The conformation of the central piperidine observed in the Akt1 crystal structure is consistent with the conformation observed previously for the initial lead **3**.[10a] Although the axial positioning of the substituents is likely to be energetically less favorable than the corresponding equatorially substituted analogue, this conformation is believed to be adopted to position the central ring substituents optimally with respect to the Akt1 binding site. It is also of note that the basic amino group forms a close contact with the sulfur of Met281[10] and hydrogen bonds with the side chain of Glu234, the backbone carbonyl of Glu278, and an associated water molecule. The pK_a of the amino group of **64** was experimentally determined and was found to have a relatively low value of 6.1. The amide NH does not form any direct contacts with the protein, although it could form a water-mediated interaction to Asp292 and Asn279. The hydroxyethyl side chain also does not appear to form any direct interactions with the protein but occupies a solvent-filled region and possibly forms a water-mediated interaction to Glu278. This residue Glu278 corresponds to Asp218 in ROCK2; consequently the presence of the hydoxyethyl group may result in a different interaction profile between the two proteins in this region. However, from the available information it is not possible to definitively explain how this group contributes to the increased potency and selectivity of this compound.

Pharmacokinetic Profiling. The DMPK profile of **64** is highlighted in Table 6. Protein binding remained low across all species, consistent with initial lead **3**. Compound **64** is extensively distributed outside of blood, with volumes of distribution ranging

Table 6. Selected DMPK Properties of Compound 64

parameter	mouse[a]	rat[b]	dog[c]	human
protein binding (free drug %)	14.3−16.7	23.5−25.1	19.2−22.9	22.3
oral bioavailability (%)	86	13	37	
blood Cl (mL·min^{-1}·kg^{-1})	207	95	22	
Vd$_{ss}$ (L/kg)	4.1	4.0	2.1	
half-life (i.v., h)	0.2	0.5	1.7	
hepatocyte Cl$_{int}$ (μL·min^{-1}·(10^6 cells)$^{-1}$)	6	32	10	1.9

[a]Alderley Park mouse. [b]Han Wistar rat. [c]Alderley Park beagle.

from 2 to 4 L/kg in preclinical species. Oral bioavailability in mouse remains high despite higher clearance, which may indicate a saturation of first-pass metabolism with the oral dose or extrahepatic metabolism. The profile in rat is somewhat worse, however: whole blood clearance is relatively high, and consequently bioavailability remains a modest 13%. Optimization of the critical parameters of cell potency, ROCK selectivity, and absolute hERG margin of **3** has been achieved, but here at the expense of some of the favorable pharmacokinetic properties the early lead demonstrated. The profile in dog appears more balanced, with moderate clearance and moderate bioavailability. As with the initial lead, in vitro intrinsic hepatic clearance (Cl$_{int}$) measured in hepatocytes is generally low, with turnover in human cells only measurable by an assay with a 2 h incubation.

Biological Activity. In order to understand the compound's selectivity profile, **64** was assayed against a larger enzyme panel of 75 kinases, of which 35 were also AGC family kinases. Significant activity, defined herein as >75% inhibition at a fixed concentration of 1 μM, was seen for just 15 kinases, of which 14 were unsurprisingly from the AGC family. In addition to Akt1−3, these were ROCK2, MKK1, MSK1, MSK2, PKCγ, PKGα, PKGβ, PRKX, RSK2, RSK3, P70S6K, and PKA. Only the latter two kinases, P70S6K and PKA, were inhibited with enzyme IC$_{50}$ values comparable to Akt1−3 inhibition, at 6 and 7 nM, respectively. However, in cellular end points of these two kinases, activity was relatively reduced compared to the primary Akt pharmacology. The cellular IC$_{50}$ against P70S6K was approximately 5 μM, as measured by inhibition of S6 phosphorylation in TSC1 null RT4 bladder cancer cells, while activity against PKA was around 1 μM, as determined by inhibition of VASP phosphorylation in A431 cells. Activity against related ROCK1 isoform was much reduced relative to ROCK2, with an IC$_{50}$ of 470 nM. Compound **64** was also very effective at inhibiting the phosphorylation of downstream Akt substrates in a

variety of cell lines (Table 7). Potent inhibition was seen against pGSK3β and pPRAS40 as direct markers of Akt cell activity. The

Table 7. Effect of 64 on Akt-Driven Cellular End Points in Various Cell Lines

marker	IC$_{50}$ (μM)		
	BT474c[a]	LNCaP[b]	MDA-MB-468[c]
pGSK3β	0.76	0.06	0.38
pPRAS40	0.31	0.22	0.39

[a]HER2+, PIK3CA mutant, breast line. [b]PTEN null, prostate line. [c]PTEN null, breast line.

growth inhibitory effect of **64** was also examined across a much larger in-house cellular panel of 182 tumor cell lines in standard proliferation assay format. Sensitive cell lines were defined as those inhibited with an IC$_{50}$ of 3 μM or less. A majority of breast cell lines proved to be sensitive (64%), with gastric, endometrial, prostate, and hematologic lines showing intermediate sensitivity (24−33% responsive). Lines that showed a poor response to **64** were derived from lung (12% sensitive), colorectal (7%), and bladder (0%) cells. The degree of sensitivity of a line could be correlated with a variety of oncogenic markers. Specifically, activating mutations in PIK3CA, loss or inactivation of tumor suppressor PTEN, or HER2 amplification all were significantly predictive of responsiveness to therapy. Additionally, correlation was also seen between the RAS mutation status of cell lines and resistance to **64**.[14]

The effect of **64** in vivo was characterized first by measuring pharmacodynamic activity in a BT474c breast adenocarcinoma xenograft model. Following single oral doses of 100 and 300 mg/kg, **64** potently inhibited the phosphorylation of Akt downstream substrates pGSK3β and pPRAS40 as well as pS6 in a manner that was directly linked to plasma exposure (Figure 4). Potent inhibition of pPRAS40 and pGSK3β was
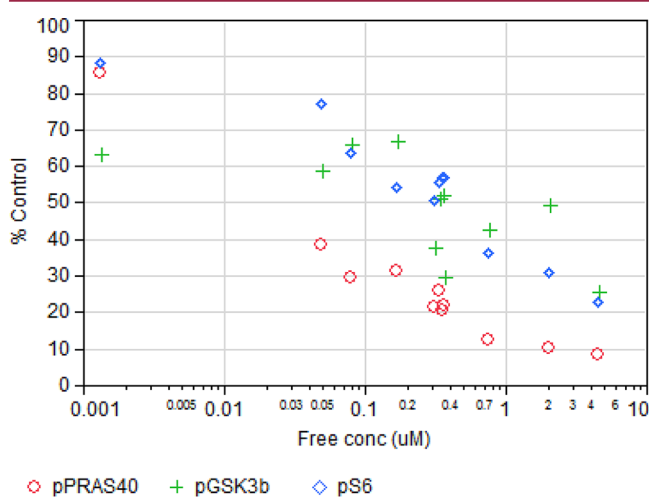
Figure 4. Pharmacodynamic activity of **64** in a BT474c xenograft model in nude mice. Concentration response was established by dosing groups at either 100 or 300 mg/kg and assaying for compound and effect at 1, 2, 4, 8, 16, and 24 h time points. Each point represents the mean of four animals.

seen out to 4 h, which started to recover at 8 h, and was back to basal levels by 24 h as compound was eliminated. The more distal cellular marker pS6 showed a similar exposure response despite overall less marked inhibition. The impact on tumor

growth of continuous oral dosing of **64** was also assessed in the same model over 14 days. When dosed at 200 mg/kg once per day, **64** was less effective than dosing at 100 mg/kg twice per day (39% inhibition versus 80%). Greatest inhibition of growth was observed with a dose of 200 mg/kg twice per day, which led to 104% inhibition, and this proved to be the maximum well-tolerated continuous twice-daily dose (Figure 5).
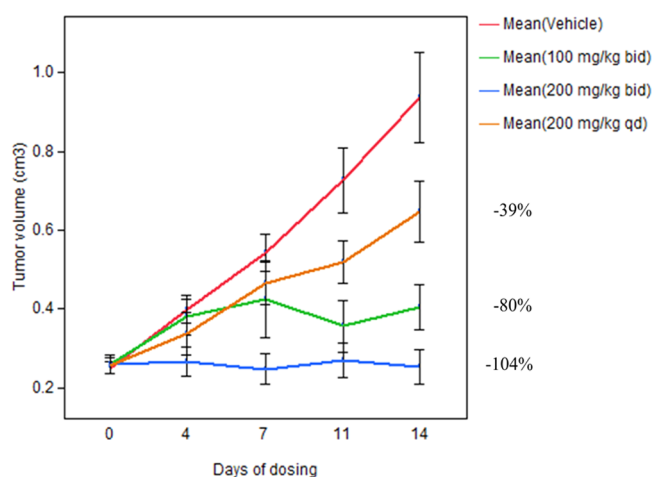
Figure 5. Activity of **64** in a BT474c tumor-bearing nude mouse disease model. Each error bar represents one standard error from the mean.

Conclusions. Compound **3** served as a lead Akt inhibitor with an acceptable DMPK profile in preclinical species and in vivo antitumor efficacy with modulation of biomarkers following oral dosing. Nevertheless, it had an unfavorably low ROCK selectivity, only modest cell activity, and unwanted activity at the hERG ion channel. A crystal structure of this compound bound to Akt1 suggested a possible vector for further substitution, and this position was ultimately explored with a range of diverse substituents and chain lengths, leading ultimately to compound **64**, AZD5363. This agent inhibits all Akt isoforms with a potency of <10 nM in vitro and is a potent inhibitor of phosphorylation of the Akt substrates GSK3β, PRAS40, and S6 in a range of cell lines. It has good selectivity over both the hERG ion channel and closely related AGC kinase ROCK, and it shows pharmacodynamic and xenograft activity in vivo. It has potential in cancer therapy and is currently in phase 1 clinical trials.

■ EXPERIMENTAL SECTION

Chemistry. All reactions were performed under inert conditions (nitrogen) unless otherwise stated. Temperatures are given in degrees Celsius (°C); operations were carried out at room or ambient temperature, that is, at a temperature in the range of 18−25 °C. All solvents and reagents were purchased from commercial sources and used without further purification. For coupling reactions, all solvents were dried and degassed prior to reaction. Reactions performed under microwave irradiation utilized either a Biotage Initiator or CEM Discover microwave. Upon workup, organic solvents were typically dried prior to concentration with anhydrous MgSO$_4$ or Na$_2$SO$_4$. Flash silica chromatography was typically performed on an Isco Companion, using Silicycle silica gel, 230−400 mesh 40−63 μm cartridges, Grace Resolv silica cartridges, or Isolute Flash Si or Si II cartridges. Reverse-phase chromatography was performed on a Waters XBridge Prep C18 optimum bed density (OBD) column (5 μm silica, 19 mm diameter, 100 mm length), with decreasingly polar mixtures of either water (containing 1% NH$_3$) and acetonitrile, or water (containing 0.1%

formic acid) and acetonitrile, as eluents. Analytical liquid chromatography−mass spectrometry (LC-MS) was performed on a Waters 2790 LC with a 996 photodiode array (PDA) detector and 2000 amu ZQ single-quadrupole mass spectrometer using a Phenomenex Gemini 50 × 2.1 mm 5 μm C18 column, or ultra-performance liquid chromatography (UPLC) was performed on an Waters Acquity binary solvent manager with Acquity PDA and an SQD mass spectrometer using a 50 × 2.1 mm 1.7 μm bridged ethyl hybrid (BEH) column from Waters, and purities were measured by UV absorption at 254 nm or by total ion chromatogram (TIC) and are ≥95% unless otherwise stated. NMR spectra were recorded on a Bruker Av400 or Bruker DRX400 spectrometer at 400 MHz in deuterated dimethyl sulfoxide (DMSO-d_6) at 303 K unless otherwise indicated. ^{1}H NMR spectra are reported as chemical shifts in parts per million (ppm) relative to an internal solvent reference. Yields are given for illustration only and are not necessarily those which can be obtained by diligent process development; preparations were repeated if more material was required.

4-(*tert*-Butoxycarbonylamino)-1-(7*H*-pyrrolo[2,3-*d*]-pyrimidin-4-yl)piperidine-4-carboxylic Acid (6). To a mixture of 4-[(2-methylpropan-2-yl)oxycarbonylamino]piperidine-4-carboxylic acid **5** (115.6 g, 473 mmol) in acetonitrile (1.5 L) and water (4.5 L) was added sodium bicarbonate (181 g, 2.2 mol), followed by 4-chloro-7*H*-pyrrolo[2,3-*d*]pyrimidine **4** (72.7 g, 473 mmol). The mixture was heated at reflux under nitrogen for 24 h and then extracted with ethyl acetate (4 × 1 L). The aqueous layer was concentrated and methanol (1.5 L) was added. The mixture was shaken for 30 min at 45 °C and filtered. The filtrate was concentrated again and dissolved in water (300 mL). HCl (6 N) was added until the pH reached 4.5 (ca. 80 mL). The mixture was filtered and the solid was dried under vacuum to afford the crude product, which was further purified by silica gel chromatography [elution with methanol/dichloromethane (DCM) 1:3] to yield the title compound **6** as a pale gray solid (105 g, 63%). ^{1}H NMR δ 1.40 (9H, s), 1.88−1.95 (2H, m), 2.02−2.06 (2H, m), 3.44−3.51 (2H, m), 4.30 (2H, d), 6.60−6.61 (1H, m), 7.16−7.18 (1H, m), 7.29 (1H, s), 8.14 (1H, s), 11.68 (1H, s); MS *m/z* MH[+] = 362.

4-Amino-*N*-[1-(4-chlorophenyl)ethyl]-1-(7*H*-pyrrolo[2,3-*d*]-pyrimidin-4-yl)piperidine-4-carboxamide (32). Compound **6** (362 mg, 1 mmol), 1-(4-chlorophenyl)ethanamine (172 mg, 1.1 mmol), *N*-(3-dimethylaminopropyl)-3-ethylcarbodiimide (231 mg, 1.5 mmol), and 1-hydroxybenzotriazole (163 mg, 1.1 mmol) were stirred together in *N*,*N*-dimethylformamide (DMF; 2 mL) under nitrogen for 16 h. The reaction mixture was partitioned between ethyl acetate (20 mL) and brine (4 × 20 mL). The organics were combined, dried, and evaporated in vacuo. The resultant white solid was dissolved in 1,4-dioxane (5 mL), and a 4 M solution of HCl in 1,4-dioxane (5 mL) was added. The resulting mixture was stirred for 16 h and then diluted with diethyl ether (50 mL). The crude product was isolated by filtration as the HCl salt, which was purified by ion-exchange chromatography on an SCX column. The desired product was eluted from the column with 7 M ammonia/methanol, and pure fractions were evaporated to dryness. This material was purified by preparative LC-MS. Fractions containing the desired compound were evaporated to dryness to afford **32** as a white solid (168 mg, 42%). ^{1}H NMR δ 1.33−1.49 (m, 5H), 1.84−2.04 (m, 2H), 2.12−2.22 (br s, 2H), 3.54 (t, 2H), 4.39 (t, 2H), 4.81−4.92 (m, 1H), 6.55−6.59 (m, 1H), 7.13−7.18 (m, 1H), 7.31−7.39 (m, 4H), 8.12 (s, 1H), 8.30 (d, 1H), 11.62 (s, 1H); HRMS *m/z* (ES+) [M + H][+] = 399.16934 (theor 399.16946).

(*R*)-4-Amino-*N*-[1-(4-chlorophenyl)ethyl]-1-(7*H*-pyrrolo[2,3-*d*]pyrimidin-4-yl)piperidine-4-carboxamide (33). In a similar manner to that described for **32**, by use of (*R*)-1-(4-chlorophenyl)-ethanamine, **33** was obtained as a white solid (53%). ^{1}H NMR δ 1.37 (3H, d), 1.39−1.48 (2H, m), 1.86−2.02 (2H, m), 2.19 (2H, s), 3.49−3.58 (2H, m), 4.34−4.43 (2H, m), 4.83−4.91 (1H, m), 6.56−6.59 (1H, m), 7.14−7.16 (1H, m), 7.32−7.38 (4H, m), 8.12 (1H, s), 8.30 (1H, d), 11.62 (1H, s); HRMS *m/z* (ES+) [M + H][+] = 399.16943 (theor 399.16946).

(*S*)-4-Amino-*N*-[1-(4-chlorophenyl)ethyl]-1-(7*H*-pyrrolo[2,3-*d*]pyrimidin-4-yl)piperidine-4-carboxamide (34). In a similar manner to that described for **32**, by use of (*S*)-1-(4-chlorophenyl)-ethanamine, **34** was obtained as a white solid (70%). ^{1}H NMR δ 1.37

(3H, d), 1.42−1.45 (2H, m), 1.88−2.01 (2H, m), 2.27 (2H, s), 3.49−3.59 (2H, m), 4.34−4.44 (2H, m), 4.83−4.90 (1H, m), 6.57−6.58 (1H, m), 7.14−7.16 (1H, m), 7.32−7.38 (4H, m), 8.12 (1H, s), 8.30 (1H, d), 11.62 (1H, s); HRMS *m/z* (ES+) [M + H][+] = 399.16946 (theor 399.16946).

4-Amino-*N*-[1-(4-chlorophenyl)propyl]-1-(7*H*-pyrrolo[2,3-*d*]-pyrimidin-4-yl)piperidine-4-carboxamide (35). In a similar manner to that described for **32**, by use of 1-(4-chlorophenyl)-propan-1-amine, **35** was obtained as a white solid (67%). ^{1}H NMR δ 0.87 (3H, t), 1.42−1.55 (2H, m), 1.72−1.79 (2H, m), 1.91−2.05 (2H, m), 2.21 (2H, s), 3.54 − 3.62 (2H, m), 4.38−4.45 (2H, m), 4.65−4.70 (1H, m), 6.61 (1H, dd), 7.18 (1H, dd), 7.32−7.37 (4H, m), 8.31 (1H, d), 8.12 (1H, s); HRMS *m/z* (ES+) [M + H][+] = 413.18515 (theor 413.18511).

4-Amino-*N*-[(4-chlorophenyl)(cyclopropyl)methyl]-1-(7*H*-pyrrolo[2,3-*d*]pyrimidin-4-yl)piperidine-4-carboxamide (36). In a similar manner to that described for **32**, by use of 1-(4-chlorophenyl)cyclopropylmethanamine (**65**, Supporting Information), **36** was obtained as a white solid (79%). ^{1}H NMR δ 0.27−0.37 (2H, m), 0.48−0.52 (2H, m), 1.18−1.24 (1H, m), 1.40−1.48 (2H, m), 1.88−2.02 (2H, m), 2.20 (2H, s), 3.50−3.59 (2H, m), 4.15 (1H, t), 4.36−4.42 (2H, m), 6.57−6.58 (1H, m), 7.14−7.16 (1H, m), 7.35−7.40 (4H, m), 8.12 (1H, s), 8.47 (1H, d), 11.62 (1H, s); HRMS *m/z* (ES+) [M + H][+] = 425.18509 (theor 425.18511).

4-Amino-*N*-[(4-chlorophenyl)(phenyl)methyl]-1-(7*H*-pyrrolo-[2,3-*d*]pyrimidin-4-yl)piperidine-4-carboxamide (37). In a similar manner to that described for **32**, by use of (4-chlorophenyl)-phenylmethanamine, **37** was obtained as a colorless solid (45%). ^{1}H NMR δ 11.65 (1H, s), 8.76 (1H, s), 8.13 (1H, s), 7.42−7.25 (9H, m), 7.17−7.15 (1H, m), 6.60−6.58 (1H, m), 6.07 (1H, s), 4.45−4.39 (2H, m), 3.59−3.51 (2H, m), 2.34−2.27 (2H, m), 2.02−1.93 (2H, m), 1.52−1.46 (2H, m); HRMS *m/z* (ES+) [M + H][+] = 461.18533 (theor 461.18511).

4-Amino-*N*-[1-(4-chlorophenyl)-2-phenylethyl]-1-(7*H*-pyrrolo[2,3-*d*]pyrimidin-4-yl)piperidine-4-carboxamide (38). In a similar manner to that described for **32**, by use of 1-(4-chlorophenyl)-2-phenylethanamine, **38** was obtained as a white solid (90%). ^{1}H NMR δ 1.21−1.42 (2H, m), 1.72−1.94 (2H, m), 2.98−3.10 (2H, m), 3.44−3.62 (2H, m), 4.13−4.23 (1H, m), 4.24−4.35 (1H, m), 4.98−5.12 (1H, m), 6.54 (1H, d), 7.12−7.29 (6H, m), 7.32−7.44 (4H, m), 8.12 (1H, s), 8.44 (1H, d), 11.63 (1H, s); HRMS *m/z* (ES+) [M + H][+] = 475.20389 (theor 475.20365).

4-Amino-*N*-(1-phenylethyl)-1-(7*H*-pyrrolo[2,3-*d*]pyrimidin-4-yl)piperidine-4-carboxamide (39). In a similar manner to that described for **32**, by use of 1-phenylethanamine, **39** was obtained as a white solid (63%). ^{1}H NMR δ 1.38 (3H, d), 1.89−2.03 (2H, m), 2.17 (2H, s), 3.50−3.57 (2H, m), 4.37−4.43 (2H, m), 4.84−4.92 (1H, m), 6.57−6.58 (1H, m), 7.15 (1H, dd), 7.19−7.26 (1H, m), 7.31−7.32 (4H, m), 8.12 (1H, s), 8.28 (1H, d), 11.62 (1H, s); HRMS *m/z* (ES+) [M + H][+] = 365.20847 (theor 365.20844).

4-Amino-*N*-[1-(4-fluorophenyl)ethyl]-1-(7*H*-pyrrolo[2,3-*d*]-pyrimidin-4-yl)piperidine-4-carboxamide (40). In a similar manner to that described for **32**, by use of 1-(4-fluorophenyl)-ethanamine, **40** was obtained as a white solid (58%). ^{1}H NMR δ 1.38 (3H, d), 1.40−1.46 (2H, m), 1.87−1.91 (1H, m), 1.96−2.01 (1H, m), 2.16 (2H, s), 3.50−3.58 (2H, m), 4.35−4.43 (2H, m), 4.84−4.92 (1H, m), 6.57−6.58 (1H, m), 7.10−7.15 (3H, m), 7.34−7.37 (2H, m), 8.12 (1H, s), 8.28 (1H, d), 11.62 (1H, s); HRMS *m/z* (ES+) [M + H][+] = 383.19894 (theor 383.19901).

4-Amino-*N*-(1-pyridin-3-ylethyl)-1-(7*H*-pyrrolo[2,3-*d*]-pyrimidin-4-yl)piperidine-4-carboxamide (41). In a similar manner to that described for **32**, by use of 1-(3-pyridyl)ethanamine, **41** was obtained as a white solid (64%). ^{1}H NMR δ 1.42 (3H, d), 1.44−1.48 (2H, m), 1.85−2.02 (2H, m), 2.20 (2H, s), 3.50−3.59 (2H, m), 4.35−4.42 (2H, m), 4.88−4.96 (1H, m), 6.57−6.58 (1H, m), 7.14−7.16 (1H, m), 7.32−7.35 (1H, m), 7.71−7.74 (1H, m), 8.12 (1H, s), 8.36 (1H, d), 8.42−8.44 (1H, m), 8.54 (1H, d), 11.62 (1H, s); HRMS *m/z* (ES+) [M + H][+] = 366.20367 (theor 366.20368).

4-Amino-*N*-(1-pyridin-2-ylethyl)-1-(7*H*-pyrrolo[2,3-*d*]-pyrimidin-4-yl)piperidine-4-carboxamide (42). In a similar manner to that described for **32**, by use of 1-(2-pyridyl)ethanamine,

42 was obtained as a white solid (38%). ^{1}H NMR (700 MHz) δ 1.36 (3H, d), 1.39−1.43 (1H, m), 1.44−1.47 (1H, m), 1.93−1.97 (1H, m), 1.98−2.03 (1H, m), 2.22 (2H, br s), 3.48−3.55 (2H, m), 4.38−4.44 (2H, m), 4.91 (1H, p), 6.56 (1H, d), 7.14 (1H, d), 7.25 (1H, ddd), 7.35 (1H, d), 7.74 (1H, td), 8.12 (1H, s), 8.52 (1H, ddd), 8.63 (1H, d), 11.62 (1H, br s); HRMS *m/z* (ES+) [M + H]$^+$ = 366.20365 (theor 366.20368).

4-Amino-*N*-{1-[4-(methylsulfonyl)phenyl]ethyl}-1-(7*H*-pyrrolo[2,3-*d*]pyrimidin-4-yl)piperidine-4-carboxamide (43). In a similar manner to that described for **32**, by use of 1-(4-methylsulfonylphenyl)ethanamine, **43** was obtained as a white solid (32%). ^{1}H NMR δ 1.42 (3H, d), 1.43−1.48 (2H, m), 1.86−2.03 (2H, m), 2.19 (2H, s), 3.19 (3H, s), 3.52−3.59 (2H, m), 4.36−4.42 (2H, m), 4.91−4.99 (1H, m), 6.57−6.58 (1H, m), 7.14−7.16 (1H, m), 7.58 (2H, d), 7.87 (2H, d), 8.12 (1H, s), 8.40 (1H, d), 11.62 (1H, s); HRMS *m/z* (ES+) [M + H]$^+$ = 443.18582 (theor 443.18599).

4-Amino-*N*-[1-(3,4-dimethoxyphenyl)ethyl]-1-(7*H*-pyrrolo-[2,3-*d*]pyrimidin-4-yl)piperidine-4-carboxamide (44). In a similar manner to that described for **32**, by use of 1-(3,4-dimethoxyphenyl)-ethanamine, **44** was obtained as a white solid (32%). ^{1}H NMR (700 MHz) δ 1.36 (3H, d), 1.39−1.45 (2H, m), 1.9−1.95 (1H, m), 1.97−2.02 (1H, m), 2.19 (2H, br s), 3.5−3.56 (2H, m), 3.71 (3H, s), 3.73 (3H, s), 4.36−4.41 (2H, m), 4.82 (1H, p), 6.56 (1H, d), 6.81 (1H, dd), 6.86 (1H, d), 6.90 (1H, d), 7.14 (1H, dd), 8.12 (1H, s), 8.20 (1H, d), 11.61 (1H, br s); HRMS *m/z* (ES+) [M + H]$^+$ = 425.22937 (theor 425.22957).

4-Amino-*N*-[1-(4-chlorophenyl)-3-(dimethylamino)propyl]-1-(7*H*-pyrrolo[2,3-*d*]pyrimidin-4-yl)piperidine-4-carboxamide (45). In a similar manner to that described for **32**, by use of 1-(4-chlorophenyl)-*N*^{3},*N*^{3}-dimethylpropane-1,3-diamine **13**, **45** was obtained as a colorless gum (70%). ^{1}H NMR (CDCl$_3$) δ 1.57 (2H, m), 1.66 (2H, br s), 1.81 (1H, m), 2.02 (1H, m), 2.18 (6H, s), 2.18−2.36 (4H, m), 3.67 (3H, m), 4.50 (2H, m), 5.00 (1H, dt), 6.52 (1H, d), 7.05 (1H, d), 7.18 (2H, d), 7.29 (2H, d), 8.33 (1H, s), 9.07 (1H, d), 9.61 (1H, s); HRMS *m/z* (ES+) [M + H]$^+$ = 456.22714 (theor 456.22731).

Amine **13** used above was obtained as described below:

3-Amino-3-(4-chlorophenyl)propan-1-ol (9). Borane−tetrahydro-furan (THF) complex (94.0 mL, 93.9 mmol) was added dropwise to a stirred suspension of 3-amino-3-(4-chlorophenyl)propionic acid **8** (2.50 g, 12.5 mmol) in THF (75 mL) at 0 °C over a period of 20 min under nitrogen. The resulting suspension was stirred at 0 °C for 30 min and then at 22 °C for 5 h. The reaction mixture was added portionwise to methanol (500 mL). The mixture was concentrated, redissolved in methanol (250 mL), and reconcentrated (this process was repeated three times). The residue was dissolved in DCM (200 mL) and washed with 1 N NaOH (150 mL). The aqueous layer was extracted with DCM (5 × 100 mL) and the extracts were combined with the organic layer. The combined organics were washed with saturated brine (2 × 150 mL), dried, and concentrated to afford a white semisolid. The crude product was purified by flash silica chromatography, elution gradient 5−7% (10:1 methanol/concentrated aqueous ammonia) in DCM. Pure fractions were evaporated to dryness to afford **9** as a white solid (1.32 g, 57%). ^{1}H NMR (CDCl$_3$) δ 1.87 (2H, m), 2.34 (2H, br s), 3.79 (2H, m), 4.13 (1H, t), 7.24 (2H, d), 7.32 (2H, d); MS *m/z* M − H$^+$ = 184.25.

tert-Butyl 1-(4-Chlorophenyl)-3-hydroxypropylcarbamate (10). Di-*tert*-butyl dicarbonate (0.705 g, 3.23 mmol) was added to **9** (0.5 g, 2.69 mmol) in DCM (30 mL) at 22 °C. The resulting solution was stirred at 22 °C for 2 h. The mixture was concentrated and the residue was purified by flash silica chromatography, elution gradient 0−4% (10:1 methanol/concentrated aqueous ammonia) in DCM. Pure fractions were evaporated to dryness to afford **10** as a white solid (0.759 g, 99%). ^{1}H NMR (CDCl$_3$) δ 1.43 (9H, s), 1.81 (1H, m), 2.04 (1H, m), 2.74 (1H, br s), 3.69 (2H, m), 4.88 (1H, br s), 5.04 (1H, d), 7.23 (2H, d), 7.32 (2H, d); MS *m/z* M$^+$ = 286.

3-(tert-Butoxycarbonylamino)-3-(4-chlorophenyl)propyl Metha-nesulfonate (11). Methanesulfonyl chloride (0.097 mL, 1.25 mmol) was added dropwise to **10** (0.326 g, 1.14 mmol) and triethylamine (0.191 mL, 1.37 mmol) in DCM (15 mL) at 22 °C. The resulting

solution was stirred at 22 °C for 2 h. The mixture was concentrated and the residue was purified by flash silica chromatography, elution gradient 20−40% ethyl acetate in isohexane. Pure fractions were evaporated to dryness to afford **11** as a white solid (0.366 g, 88%). ^{1}H NMR (CDCl$_3$) δ 1.42 (9H, s), 2.19 (2H, m), 3.01 (3H, s), 4.24 (2H, m), 4.82 (2H, m), 7.22 (2H, d), 7.33 (2H, d); MS *m/z* M$^+$ = 364.

tert-Butyl 1-(4-Chlorophenyl)-3-(dimethylamino)propylcarbamate (12). Compound **11** (0.075 g, 0.21 mmol) and tetra-*n*-butylammonium iodide (0.015 g, 0.04 mmol) were dissolved in a solution of dimethylamine in THF (2M, 5.15 mL, 10.3 mmol) and sealed into a microwave tube. The reaction was heated to 150 °C for 30 min in the microwave reactor and cooled to ambient temperature. The reaction mixture was concentrated, diluted with DCM (25 mL), and washed with water (25 mL). The organic layer was filtered through a phase-separating filter paper and evaporated. The crude product was purified by flash silica chromatography, elution gradient 4−8% (10:1 methanol/concentrated aqueous ammonia) in DCM. Pure fractions were evaporated to dryness to afford **12** as a colorless oil (0.054 mg, 84%). ^{1}H NMR (CDCl$_3$) δ 1.40 (9H, s), 1.80 (1H, br s), 1.94 (1H, m), 2.23 (6H, s), 2.26 (2H, m), 4.71 (1H, br s), 6.16 (1H, br s), 7.21 (2H, d), 7.29 (2H, d); MS *m/z* MH$^+$ = 313.

1-(4-Chlorophenyl)-N^3,N^3-dimethylpropane-1,3-diamine (13). Hydrogen chloride (4 M in 1,4-dioxane, 1.13 mL, 32.6 mmol) was added to **12** (0.051 g, 0.16 mmol) in a mixture of DCM (5 mL) and methanol (2 mL) at 22 °C. The resulting solution was stirred at 22 °C for 4 h. The mixture was concentrated and the residue was purified by ion-exchange chromatography on an SCX column. The desired product was eluted from the column with 2 M ammonia/methanol, and pure fractions were evaporated to dryness to afford **13** as a colorless oil (0.032 g, 92%). ^{1}H NMR (CDCl$_3$) δ 1.72−1.85 (2H, m), 2.19−2.32 (2H, m), 2.21 (6H, s), 3.99 (1H, t), 7.25−7.31 (4H, m); MS *m/z* MH$^+$ = 213.

4-Amino-*N*-[1-(4-chlorophenyl)-4-(dimethylamino)butyl]-1-(7*H*-pyrrolo[2,3-*d*]pyrimidin-4-yl)piperidine-4-carboxamide (46). In a similar manner to that described for **32**, by use of 1-(4-chlorophenyl)-*N*^{4},*N*^{4}-dimethylbutane-1,4-diamine (**71**, Supporting Information), **46** was obtained as a white solid (36%). ^{1}H NMR δ 1.26−1.33 (2H, m), 1.38−1.47 (2H, m), 1.65−1.75 (2H, m), 1.87−2.01 (2H, m), 2.08 (6H, s), 2.18 (2H, t), 3.50−3.58 (2H, m), 4.35−4.41 (2H, m), 4.73 (1H, m), 6.57 (1H, d), 7.14−7.16 (1H, m), 7.32−7.37 (4H, m), 8.12 (1H, s), 8.31 (1H, d), 11.62 (1H, s); HRMS *m/z* (ES+) [M + H]$^+$ = 470.24261 (theor 470.24296).

4-Amino-*N*-[1-(4-chlorophenyl)-4-pyrrolidin-1-ylbutyl]-1-(7*H*-pyrrolo[2,3-*d*]pyrimidin-4-yl)piperidine-4-carboxamide (47). In a similar manner to that described for **32**, by use of 1-(4-chlorophenyl)-4-(pyrrolidin-1-yl)butan-1-amine (**74**, Supporting Information), **47** was obtained as a white solid (12%). ^{1}H NMR δ 1.31−1.49 (4H, m), 1.65 (4H, s), 1.69−1.77 (2H, m), 1.88−1.98 (2H, m), 2.15 (2H, s), 2.34 (4H, s), 2.36 (2H, s), 3.53−3.58 (2H, m), 4.34−4.41 (2H, m), 4.73 (1H, m), 6.57 (1H, d), 7.14−7.15 (1H, d), 7.32−7.37 (4H, m), 8.12 (1H, s), 8.30 (1H, d), 11.62 (1H, s); HRMS *m/z* (ES+) [M + H]$^+$ = 496.25839 (theor 496.25861).

4-Amino-*N*-[1-(4-chlorophenyl)-4-morpholin-4-ylbutyl]-1-(7*H*-pyrrolo[2,3-*d*]pyrimidin-4-yl)piperidine-4-carboxamide (48). In a similar manner to that described for **32**, by use of 1-(4-chlorophenyl)-4-morpholinobutan-1-amine (**72**, Supporting Information), **48** was obtained as a white solid (3%). ^{1}H NMR δ 1.32−1.37 (1H, m), 1.44−1.51 (1H, m), 1.57−1.76 (4H, m), 2.10−2.17 (2H, m), 2.26−2.35 (6H, m), 3.47−3.56 (6H, m), 4.51 (2H, d), 4.79 (1H, m), 6.62−6.64 (1H, m), 7.19 (1H, t), 7.32−7.34 (2H, d), 7.37−7.39 (2H, d), 8.16 (1H, s), 8.49 (1H, s), 11.68 (1H, s); HRMS *m/z* (ES+) [M + H]$^+$ = 512.25324 (theor 512.25353).

4-Amino-*N*-[1-(4-chlorophenyl)-4-piperidin-1-ylbutyl]-1-(7*H*-pyrrolo[2,3-*d*]pyrimidin-4-yl)piperidine-4-carboxamide (49). In a similar manner to that described for **32**, by use of 1-(4-chlorophenyl)-4-(piperidin-1-yl)butan-1-amine (**73**, Supporting Information), **49** was obtained as a white solid (17%). ^{1}H NMR δ 1.31−1.37 (3H, m), 1.41−1.47 (6H, m), 1.66−1.73 (2H, m), 1.86−2.00 (2H, m), 2.16−2.24 (7H, m), 3.50−3.58 (2H, m), 4.34−4.40 (2H, m), 4.73 (1H, m), 6.57 (1H, d), 7.15 (1H, d), 7.31−7.37 (4H,

m), 8.12 (1H, s), 8.29 (1H, d), 11.62 (1H, s); HRMS m/z (ES+) $[M + H]^+$ = 510.27451 (theor 510.27426).

(S)-4-Amino-N-[1-(4-chlorophenyl)-3-(dimethylamino)-propyl]-1-(7H-pyrrolo[2,3-d]pyrimidin-4-yl)piperidine-4-carboxamide (50). Racemic **45** was chirally separated on a Chiralpak AD-H supercritical fluid chromatography (SFC; 250 mm × 20 mm) column, using SFC, elution solvent 7:3 CO_2/(ethanol + 0.1% diethylamine, DEA). The appropriate fractions for the first eluted isomer were evaporated and the residue was triturated with diethyl ether to give **50** as a white solid (25%). ¹H NMR (CDCl₃) δ 1.57 (2H, m), 1.66 (2H, br s), 1.81 (1H, m), 2.02 (1H, m), 2.18 (6H, s), 2.18−2.36 (4H, m), 3.67 (3H, m), 4.50 (2H, m), 5.00 (1H, dt), 6.52 (1H, d), 7.05 (1H, d), 7.18 (2H, d), 7.29 (2H, d), 8.33 (1H, s), 9.07 (1H, d), 9.61 (1H, s); HRMS m/z (ES+) $[M + H]^+$ = 456.22723 (theor 456.22731).

4-Amino-N-[(1S)-1-(4-chlorophenyl)-3-pyrrolidin-1-ylpropyl]-1-(7H-pyrrolo[2,3-d]pyrimidin-4-yl)piperidine-4-carboxamide (51). In a similar manner to that described for **32**, by use of 1-(4-chlorophenyl)-4-(pyrrolidin-1-yl)butan-1-amine (**85**, Supporting Information), **51** was obtained as a white solid (10%). ¹H NMR δ 1.42−1.58 (2H, m), 1.71 (5H, s), 1.84−2.02 (5H, m), 2.33 (2H, m), 2.55 (2H, m), 3.51−3.59 (2H, m), 4.36−4.43 (2H, m), 4.86 (1H, t), 6.58 (1H, d), 7.16 (1H, d), 7.30−7.38 (5H, m), 8.12 (1H, s), 11.63 (1H, s); HRMS m/z (ES+) $[M + H]^+$ = 482.24289 (theor 482.24296).

4-Amino-N-[(1S)-1-(4-chlorophenyl)-3-piperidin-1-ylpropyl]-1-(7H-pyrrolo[2,3-d]pyrimidin-4-yl)piperidine-4-carboxamide (52). In a similar manner to that described for **32**, by use of 1-(4-chlorophenyl)-4-(piperidin-1-yl)butan-1-amine (**84**, Supporting Information), **52** was obtained as a white solid (17%). ¹H NMR δ 1.33−1.50 (8H, m), 1.82−1.90 (4H, m), 2.15 (2H, t), 2.25−2.34 (4H, m), 3.53−3.57 (2H, m), 4.39 (2H, m), 4.82 (1H, m), 6.57 (1H, d), 7.14−7.16 (1H, d), 7.30−7.37 (4H, m), 8.12 (1H, s), 8.64−8.66 (1H, d), 11.62 (1H, s); HRMS m/z (ES+) $[M + H]^+$ = 496.25900 (theor 496.25861).

4-Amino-N-[2-amino-1-(4-chlorophenyl)-2-oxoethyl]-1-(7H-pyrrolo[2,3-d]pyrimidin-4-yl)piperidine-4-carboxamide (53). In a similar manner to that described for **32**, by use of 2-amino-2-(4-chlorophenyl)acetamide, **53** was obtained as a white solid (92%). ¹H NMR δ 11.65 (1H, s), 8.92 (1H, s), 8.13 (1H, s), 7.80 (1H, s), 7.45−7.39 (4H, m), 7.29 (1H, s), 7.17−7.15 (1H, m), 6.58−6.57 (1H, m), 5.30 (1H, s), 4.48−4.38 (2H, m), 3.55−3.46 (2H, m), 2.43 (2H, s), 2.03−1.94 (1H, m), 1.90−1.82 (1H, m), 1.49−1.39 (2H, m); HRMS m/z (ES+) $[M + H]^+$ = 428.15979 (theor 428.15963).

N-[2-Acetamido-1-(4-chlorophenyl)ethyl]-4-amino-1-(7H-pyrrolo[2,3-d]pyrimidin-4-yl)piperidine-4-carboxamide (55). In a similar manner to that described for **32**, by use of N-[2-amino-2-(4-chlorophenyl)ethyl]acetamide **25**, **55** was obtained as a cream film (81%). ¹H NMR δ 1.43 (2H, t), 1.79 (3H, s), 1.83−2.04 (2H, m), 2.20 (2H, br s), 3.32−3.38 (2H, m), 3.58 (2H, q), 4.32−4.42 (2H, m), 4.82−4.88 (1H, m), 6.56−6.60 (1H, m), 7.14−7.18 (1H, m), 7.33 (2H, d), 7.38 (2H, d), 7.94 (1H, t), 8.13 (1H, s), 8.42−8.50 (1H, m), 11.63 (1H, s); HRMS m/z (ES+) $[M + H]^+$ = 456.19113 (theor 456.19093).

The amine **25** used above was synthesized as described below:

tert-Butyl 2-Acetamido-1-(4-chlorophenyl)ethylcarbamate (24). A solution of **23** (0.208 g, 0.77 mmol) and N,N-diisopropylethylamine (DIPEA; 0.266 mL, 1.54 mmol) in THF (5 mL) was treated with acetic anhydride (0.102 mL, 1.08 mmol). The resulting solution was stirred at ambient temperature for 2 h. The mixture was partitioned between DCM and sodium bicarbonate solution. The organic layer was concentrated and the residue was purified by flash column chromatography on silica with gradient elution (10−40% ethyl acetate/DCM) to afford **24** as a colorless solid (0.15 g, 63%). ¹H NMR (CDCl₃) δ 1.41 (9H, s), 1.98 (3H, s), 3.46−3.67 (2H, m), 4.74 (1H, br s), 4.97−5.56 (1H, m), 5.89 (1H, br s), 7.22 (2H, d), 7.32 (2H, d); MS m/z MH⁺ = 313.

N-[2-Amino-2-(4-chlorophenyl)ethyl]acetamide (25). Compound **24** (148 mg, 0.47 mmol) was treated with TFA (2 mL). The solution was stirred for 1 h at room temperature. The mixture was concentrated under reduced pressure. The crude product was purified by ion-exchange chromatography on an SCX column. The residue was loaded onto the column in methanol and washed with methanol. The desired product was eluted from the column with 2 M ammonia in methanol, and pure fractions were evaporated to dryness to afford **25** as a pale yellow crystalline solid (98 mg, 97%). ¹H NMR (CDCl₃) δ 1.61 (2H, br s), 1.97 (3H, s), 3.28−3.37 (1H, m), 3.44−3.52 (1H, m), 4.05−4.11 (1H, m), 5.78 (1H, br s), 7.28−7.36 (4H, m); MS m/z MH⁺ = 213.

4-Amino-N-[1-(4-chlorophenyl)-2-sulfamoylethyl]-1-(7H-pyrrolo[2,3-d]pyrimidin-4-yl)piperidine-4-carboxamide (56). In a similar manner to that described for **32**, by use of 2-amino-2-(4-chlorophenyl)ethanesulfonamide **22**, **56** was obtained as a colorless solid (84%). ¹H NMR δ 1.35−1.53 (2H, m), 1.86−2.04 (2H, m), 3.35−3.40 (1H, m), 3.52−3.62 (2H, m), 3.68 (1H, dd), 4.33−4.41 (2H, m), 5.24−5.29 (1H, m), 6.56−6.60 (1H, m), 6.88 (2H, s), 7.13−7.17 (1H, m), 7.39 (4H, s), 8.13 (1H, s), 8.68 (1H, br s), 11.63 (1H, s); HRMS m/z (ES+) $[M + H]^+$ = 478.14221 (theor 478.14226).

The amine **22** used above was synthesized as described below:

2-(tert-Butoxycarbonylamino)-2-(4-chlorophenyl)ethyl Ethanethioate (19). A solution of **18** (600 mg, 1.72 mmol) in DMF (10 mL) was treated with potassium thioacetate (392 mg, 3.43 mmol), and the mixture was heated at 50 °C for 1 h. The mixture was cooled and partitioned between ethyl acetate and water. The organic layer was washed twice with water and then dried and concentrated to dryness. The residue was purified by flash column chromatography on silica with gradient elution (10−20% ethyl acetate/isohexane) to give **19** as a cream crystalline solid (509 mg, 90%). ¹H NMR (CDCl3) δ 1.40 (9H, s), 2.35 (3H, s), 3.15−3.28 (2H, m), 4.78 (1H, br s), 5.07 (1H, br s), 7.24 (2H, d), 7.31 (2H, d); MS m/z $[M - H - CH_3CO]^-$ = 286.

tert-Butyl 1-(4-Chlorophenyl)-2-(chlorosulfonyl)ethylcarbamate (20). N-Chlorosuccinimide (819 mg, 6.14 mmol) was added to a solution of 2 M hydrochloric acid (0.8 mL) in acetonitrile (10 mL). The reaction flask was cooled with an ice bath to 10 °C, and **19** (506 mg, 1.53 mmol) was added portionwise. The mixture warmed during the addition and was stirred for 10 min at room temperature. The mixture was partitioned between ethyl acetate and water. The organic layer was washed with brine, dried, and concentrated to dryness to afford **20** as a colorless solid (602 mg, 100%). ¹H NMR (CDCl₃) δ 1.44 (9H, s), 2.77 (1H, s), 4.06 (1H, dd), 4.36 (1H, br s), 5.15−5.23 (1H, m), 5.29−5.37 (1H, m), 7.29 (2H, d), 7.38 (2H, d).

tert-Butyl 1-(4-Chlorophenyl)-2-sulfamoylethylcarbamate (21). Ammonia (1.5 mL, 31.50 mmol) was added to a suspension of **20** (0.542 g, 1.53 mmol) in acetonitrile (10 mL). The mixture was stirred for 16 h at room temperature. The mixture was partitioned between ethyl acetate and water and the organic layer was washed with brine. The organic solution was dried and concentrated under reduced pressure. The residue was purified by flash column chromatography on silica with gradient elution (10−30% ethyl acetate/DCM) to afford **21** as a colorless solid (0.35 g, 69%). ¹H NMR δ 1.36 (9H, s), 3.21−3.28 (1H, m), 3.47−3.56 (1H, m), 5.02 (1H, br s), 6.88 (2H, s), 7.35 (2H, d), 7.41 (2H, d), 7.49−7.60 (1H, m); MS m/z $[M - H]^-$ = 333.

2-Amino-2-(4-chlorophenyl)ethanesulfonamide (22). Compound **21** (325 mg, 0.97 mmol) was treated with trifluoroacetic acid (TFA; 8 mL). The resulting solution was stirred for 15 min at room temperature. The mixture was concentrated under reduced pressure and the residue was purified by ion-exchange chromatography on an SCX column. The column was washed with methanol, the desired product was eluted with ammonia in methanol (2 M), and pure fractions were evaporated to dryness to afford **22** as a colorless solid (221 mg, 97%). ¹H NMR δ 3.13−3.25 (2H, m), 4.39 (1H, dd), 7.35−7.48 (4H, m); MS m/z $[M - H]^-$ = 233.

4-Amino-N-[1-(4-chlorophenyl)-3-sulfamoylpropyl]-1-(7H-pyrrolo[2,3-d]pyrimidin-4-yl)piperidine-4-carboxamide (57). In a similar manner to that described for **32**, by use of 3-amino-3-(4-chlorophenyl)propane-1-sulfonamide (**81**, Supporting Information), **57** was obtained as a colorless gum (32%). ¹H NMR δ 1.48 (2H, m), 1.90−2.06 (2H, m), 2.09−2.24 (2H, m), 2.87 (1H, ddd), 3.02 (1H, ddd), 3.56 (2H, m), 3.56 (2H, d), 4.41 (2H, m), 4.91 (1H, br s), 6.59 (1H, dd), 6.80 (2H, s), 7.16 (1H, dd), 7.38−7.43 (4H, m), 8.13 (1H, s), 8.46 (1H, s), 11.64 (1H, s); HRMS m/z (ES+) $[M + H]^+$ = 492.15775 (theor 492.15791).

4-Amino-*N*-[1-(4-chlorophenyl)-2-sulfamoylethyl]-1-(7*H*-pyrrolo[2,3-*d*]pyrimidin-4-yl)piperidine-4-carboxamide (58). In a similar manner to that described for **32**, by use of *N*-[2-amino-2-(4-chlorophenyl)ethyl]methanesulfonamide **27**, **58** was obtained as a colorless solid (75%). ^{1}H NMR δ 1.38−1.53 (2H, m), 1.85−2.07 (2H, m), 2.20 (2H, br s), 2.85 (3H, s), 3.57 (2H, m), 4.34−4.46 (2H, m), 4.87−4.94 (1H, m), 6.57−6.60 (1H, m), 7.12−7.19 (2H, m), 7.35−7.43 (4H, m), 8.13 (1H, s), 8.46 (1H, br s), 11.64 (1H, s); HRMS *m/z* (ES+) [M + H]+ = 492.15784 (theor 492.15791).

Amine **27** used above was synthesized as described below:

tert-Butyl 1-(4-Chlorophenyl)-2-hydroxyethylcarbamate (17). 2-Amino-2-(4-chlorophenyl)acetic acid (12 g, 64.65 mmol) was stirred in THF (200 mL), and sodium borohydride (5.82 g, 153.87 mmol) was added in portions to the stirred mixture under nitrogen. A solution of iodine (16.41 g, 64.65 mmol) in THF (20 mL) was added dropwise while the temperature was maintained below 15 °C by use of an ice bath. The resulting mixture was warmed to room temperature and stirred at reflux overnight. The reaction was quenched by the addition of methanol (40 mL) and then treated with triethylamine (18.02 mL, 129 mmol) and di-*tert*-butyl dicarbonate (14.11 g, 65 mmol). The mixture was stirred for 2 h at room temperature before being partitioned between ethyl acetate and water. The organic layer was dried and concentrated under reduced pressure. The residue was purified by flash silica chromatography with gradient elution (10−50% ethyl acetate/DCM) to afford **17** as a colorless solid (10.32 g, 59%). ^{1}H NMR δ 1.37 (9H, s), 3.41−3.52 (2H, m), 4.42−4.58 (1H, m), 4.79 (1H, t), 7.23 (1H, d), 7.31 (2H, d), 7.37 (2H, d).

2-(tert-Butoxycarbonylamino)-2-(4-chlorophenyl)ethyl Methanesulfonate (18). Methanesulfonyl chloride (1.45 mL, 19 mmol) was added to **17** (4.63 g, 17 mmol) and DIPEA (6.23 mL, 35.78 mmol) in DCM (40 mL) cooled to 0 °C over a period of 5 min under nitrogen. The resulting solution was stirred at 20 °C for 2 h. The reaction mixture was diluted with DCM (100 mL) and washed sequentially with water (100 mL). The organic layer was dried and evaporated to afford crude product, which was purified by flash silica chromatography, elution gradient 0−10% ethyl acetate in DCM. Pure fractions were evaporated to dryness to afford **18** as a white solid (3.12 g, 52%). ^{1}H NMR δ 1.39 (9H, s), 3.17 (3H, s), 4.22−4.28 (2H, m), 4.90 (1H, d), 7.40−7.46 (4H, m), 7.68 (1H, d). *m/z* (ESI+) [M − H]− = 348.

tert-Butyl 2-amino-1-(4-chlorophenyl)ethylcarbamate (23). A solution of **18** (535 mg, 1.53 mmol) in DMF (8 mL) was treated with sodium azide (199 mg, 3.06 mmol), and the mixture was heated at 80 °C for 1 h. The mixture was cooled and allowed to stir at room temperature overnight. The solution was partitioned between ethyl acetate and water. The organic layer was washed twice with water and then dried and concentrated until the final volume was approximately 5 mL. Ethanol (20 mL) and 10% palladium on carbon (75 mg, 0.07 mmol) were added. The resulting suspension was stirred under an atmosphere of hydrogen at ambient pressure and temperature for 1 h. The mixture was filtered and the filtrate was concentrated under reduced pressure to give **23** as a gum (410 mg, 99%), which was used without further purification. MS *m/z* MH+ = 271.

tert-Butyl 1-(4-Chlorophenyl)-2-(methylsulfonamido)ethylcarbamate (26). A solution of **23** (220 mg, 0.81 mmol) and DIPEA (0.28 mL, 1.63 mmol) in THF (5 mL) was treated with methanesulfonyl chloride (0.075 mL, 0.98 mmol). The resulting solution was stirred at ambient temperature for 2 h. The mixture was partitioned between DCM and sodium bicarbonate solution. The organic layer was concentrated and the residue was purified by flash column chromatography on silica with gradient elution (10−30% ethyl acetate/DCM) to afford **26** as a colorless solid (154 mg, 54%). ^{1}H NMR (CDCl₃) δ 1.43 (9H, s), 2.92 (3H, s), 3.38−3.52 (2H, m), 4.68−4.84 (2H, m), 5.20−5.28 (1H, m), 7.23 (2H, d), 7.35 (2H, d); MS *m/z* [M − H]− = 347.

N-[2-Amino-2-(4-chlorophenyl)ethyl]methanesulfonamide (27). Compound **26** (151 mg, 0.43 mmol) was treated with TFA (2 mL). The solution was stirred for 1 h at room temperature and then concentrated under reduced pressure. The crude product was purified by ion-exchange chromatography on an SCX column. The residue was loaded onto the column in methanol and washed with methanol. The desired product was eluted from the column with 2 M ammonia in

methanol, and pure fractions were evaporated to dryness to afford **27** as a colorless crystalline solid (93 mg, 86%). ^{1}H NMR (CDCl₃) δ 2.89 (3H, s), 3.17 (1H, dd), 3.33 (1H, dd), 4.12 (1H, dd), 4.74 (1H, br s), 7.29 (2H, d), 7.34 (2H, d); MS *m/z* [M − H]− = 247.

4-Amino-*N*-[1-(4-chlorophenyl)-3-(methylsulfonamido)-propyl]-1-(7*H*-pyrrolo[2,3-*d*]pyrimidin-4-yl)piperidine-4-carboxamide (59). In a similar manner to that described for **32**, by use of *N*-[3-amino-3-(4-chlorophenyl)propyl]methanesulfonamide **31**, **59** was obtained as a white solid (65%). ^{1}H NMR δ 1.40−1.48 (2H, m), 1.86−1.90 (2H, m), 1.93−1.97 (2H, m), 2.17 (2H, s), 2.88 (3H, s), 2.93−2.97 (2H, m), 3.53−3.60 (2H, m), 4.37 (2H, t), 4.87 (1H, d), 6.57−6.59 (1H, m), 7.00 (1H, t), 7.15−7.16 (1H, m), 7.35−7.40 (4H, m), 8.13 (1H, s), 8.38 (1H, d), 11.63 (1H, s); HRMS *m/z* (ES+) [M + H]+ = 506.17361 (theor 506.17356).

The amine **31** used above was synthesized as described below:

tert-Butyl 1-(4-Chlorophenyl)-2-cyanoethylcarbamate (28). Sodium cyanide (105 mg, 2.14 mmol) was added to **18** (300 mg, 0.86 mmol) in DMF (5 mL) at 20 °C. The resulting suspension was stirred at 80 °C for 3 h. The reaction mixture was evaporated to dryness and redissolved in water (10 mL) and then washed sequentially with DCM (3 × 10 mL). The organic layer was dried and evaporated to afford crude product, which was purified by flash silica chromatography, elution gradient 0−25% ethyl acetate in isohexane, to afford **28** as a white solid (209 mg, 87%). ^{1}H NMR δ 1.38−1.42 (9H, s), 2.82−2.89 (2H, m), 4.89 (1H, d), 7.38−7.45 (4H, m), 7.76 (1H, d); *m/z* (ESI+) [M − H]− = 279.

tert-Butyl 3-Amino-1-(4-chlorophenyl)propylcarbamate (29). Lithium aluminum hydride (1 M in THF, 0.71 mL, 0.71 mmol) was added dropwise to **28** (200 mg, 0.71 mmol) in THF (4 mL) at 20 °C under nitrogen. The resulting solution was stirred at 20 °C for 2 h. The reaction mixture was quenched with aqueous NaOH (1 M, 1 mL) and the solution was filtered. The solution was diluted with ethyl acetate (20 mL), and washed with water (2 × 10 mL). The organic layer was dried and evaporated to afford **29** as a gum (203 mg, 100%), which was used without further purification. *m/z* (ESI+) [M + H]+ = 285.

tert-Butyl 1-(4-Chlorophenyl)-3-(methylsulfonamido)propylcarbamate (30). Methanesulfonyl chloride (0.082 mL, 1.05 mmol) was added dropwise to **29** (300 mg, 1.05 mmol) and DIPEA (0.367 mL, 2.11 mmol) in DCM (4 mL) at 20 °C. The resulting solution was stirred at 20 °C for 18 h. The reaction mixture was concentrated and diluted with diethyl ether (25 mL) and washed with water (25 mL). The organic layer was dried and evaporated to afford crude product. The crude product was purified by flash silica chromatography, elution gradient 0−20% ethyl acetate in DCM. Pure fractions were evaporated to dryness to afford **30** as a white solid (275 mg, 72%). ^{1}H NMR δ 1.37 (9H, s), 1.76 (1H, m), 1.82−1.88 (1H, m), 2.87 (3H, s), 2.89−2.91 (2H, m), 4.58 (1H, d), 7.00 (1H, t), 7.32 (2H, d), 7.39 (2H, d), 7.48 (1H, d); *m/z* (ESI+) [M + H]+ = 361.

N-[3-Amino-3-(4-chlorophenyl)propyl]methanesulfonamide (31). TFA (4 mL) was added to **30** (275 mg, 0.76 mmol) and the mixture was stirred at 20 °C for 2 h. The reaction was concentrated and the residue was purified by ion-exchange chromatograph on an SCX column. The desired product was eluted from the column with 7 N ammonia in methanol to afford **31** as a colorless gum (113 mg, 57%). ^{1}H NMR δ 1.69−1.72 (2H, m), 2.87 (3H, s), 2.94−2.98 (2H, m), 3.18−3.19 (1H, m), 3.87 (1H, t), 7.35−7.40 (4H, m); *m/z* (ESI+) [M + H]+ = 262.

4-Amino-*N*-[1-(4-chlorophenyl)-2-hydroxyethyl]-1-(7*H*-pyrrolo[2,3-*d*]pyrimidin-4-yl)piperidine-4-carboxamide (60). In a similar manner to that described for **32**, by use of 2-amino-2-(4-chlorophenyl)ethanol (see US2006/0004045 for preparation), **32** was obtained as a colorless crystalline solid (80%). ^{1}H NMR δ 1.40−1.49 (2H, m), 1.85−2.09 (2H, m), 3.48−3.69 (4H, m), 4.35−4.48 (2H, m), 4.72−4.81 (1H, m), 4.90−4.96 (1H, m), 6.58 (1H, br s), 7.12−7.18 (1H, m), 7.30−7.40 (4H, m), 8.13 (1H, s), 8.45−8.53 (1H, m), 11.64 (1H, s); HRMS *m/z* (ES+) [M + H]+ = 415.16461 (theor 415.16438).

4-Amino-*N*-[1-(4-chlorophenyl)-4-hydroxybutyl]-1-(7*H*-pyrrolo[2,3-*d*]pyrimidin-4-yl)piperidine-4-carboxamide (62). In a similar manner to that described for **32**, by use of 4-amino-4-(4-chlorophenyl)butan-1-ol (**68**, Supporting Information), **62** was

obtained as a colorless solid (34%). ^{1}H NMR δ 1.28−1.51 (4H, m), 1.69−1.80 (2H, m), 1.90−2.03 (2H, m), 3.37−3.41 (2H, m), 3.50−3.58 (2H, m), 4.37−4.43 (3H, m), 4.71−4.76 (1H, m), 6.59 (1H, m), 7.16 (1H, m), 7.36 (4H, m), 8.13 (1H, s), 8.33 (1H, d), 11.64 (1H, s); HRMS m/z (ES+) $[M + H]^+$ = 443.19553 (theor 443.19568).

4-Amino-N-[1-(4-chlorophenyl)-3-methoxypropyl]-1-(7H-pyrrolo[2,3-d]pyrimidin-4-yl)piperidine-4-carboxamide (63). In a similar manner to that described for **32**, by use of 1-(4-chlorophenyl)-3-methoxypropan-1-amine **15**, **63** was obtained as a white solid (66%). ^{1}H NMR δ 1.44 (2H, m), 1.88−2.02 (5H, m), 2.46 (2H, s), 3.21 (3H, s), 3.28 (2H, t), 3.55 (2H, m), 4.39 (2H, m), 4.87 (1H, dt), 6.59 (1H, dd), 7.16 (1H, dd), 7.33 (2H, d), 7.37 (2H, d), 8.13 (1H, s), 8.45 (1H, d), 11.63 (1H, s); HRMS m/z (ES+) $[M + H]^+$ = 443.19592 (theor 443.19568).

The amine **15** used above was synthesized as described below:

tert-Butyl 1-(4-Chlorophenyl)-3-methoxypropylcarbamate (14). Sodium hydride (35 mg, 0.87 mmol) was added to **10** (200 mg, 0.70 mmol) in THF (10 mL) at 0 °C under nitrogen. The mixture was stirred at 0 °C for 15 min. Methyl iodide (0.044 mL, 0.70 mmol) was added dropwise, and the resulting suspension was stirred at 22 °C for 4 h. The reaction was quenched with potassium bisulfate solution (1M, 0.5 mL) and water (15 mL). The mixture was extracted with diethyl ether (3 × 20 mL), and the combined extracts were washed with saturated brine (20 mL), dried, and evaporated to give crude product. The crude product was purified by flash silica chromatography, elution gradient 20−60% ethyl acetate in isohexane, to afford **14** as a white solid (80 mg, 38%). ^{1}H NMR (CDCl$_3$) δ 1.40 (9H, s), 1.91 (1H, s), 2.01 (1H, s), 3.30 (3H, s), 3.32 (2H, m), 4.79 (1H, br s), 5.45 (1H, br s), 7.20 (2H, d), 7.29 (2H, d); m/z (ESI+) $[M + H]^+$ = 300.

1-(4-Chlorophenyl)-3-methoxypropan-1-amine (15). Hydrogen chloride (4 M in 1,4-dioxane, 0.667 mL, 2.67 mmol) was added to **14** (80 mg, 0.27 mmol) in a mixture of DCM (5 mL) and methanol (2 mL) at 22 °C. The resulting solution was stirred at 22 °C for 5 h. The mixture was concentrated and the residue was purified by ion-exchange chromatography on an SCX column. The desired product was eluted from the column with 2 M ammonia in methanol, and pure fractions were evaporated to dryness to afford **15** as a colorless oil (47 mg, 88%). ^{1}H NMR (CDCl$_3$) δ 1.80−1.96 (2H, m), 3.31 (3H, s), 3.32 (1H, m), 3.43 (1H, m), 4.09 (1H, t), 7.27−7.31 (4H, m); m/z (ESI+) $[M + H]^+$ = 200.

(S)-4-Amino-N-[1-(4-chlorophenyl)-3-hydroxypropyl]-1-(7H-pyrrolo[2,3-d]pyrimidin-4-yl)piperidine-4-carboxamide, AZD5363 (64). In a similar manner to that described for **32**, by use of (S)-3-amino-3-(4-chlorophenyl)propan-1-ol (**75**, Supporting Information), **64** was obtained as a white solid (25%). ^{1}H NMR δ 1.45 (2H, d), 1.86 (1H, d), 1.90−1.93 (1H, m), 2.19 (2H, s), 3.38 (2H, q), 3.51−3.58 (2H, m), 4.35−4.38 (2H, m), 4.53 (1H, t), 4.88 (1H, d), 6.58 (1H, t), 7.16 (1H, t), 7.32−7.38 (4H, m), 8.12 (1H, s), 8.43 (1H, d), 11.63 (1H, s); HRMS m/z (ES+) $[M + H]^+$ = 429.17978 (theor 429.18003). The chiral purity of **64** was assessed by use of a 5 μm Chiralpak IA (250 mm × 4.6 mm) GB012 column with isohexane/ethanol/triethylamine (50/50/0.1) as eluent, and it was determined to contain <0.1% of the other enantiomer.

ASSOCIATED CONTENT

Ⓢ Supporting Information

Additional text with details of the full synthesis and spectroscopic characterization of all additional compounds and intermediate, together with all protocols for in vitro and in vivo experiments, and one table listing crystallographic information. This material is available free of charge via the Internet at http://pubs.acs.org.

AUTHOR INFORMATION

Corresponding Author

*Telephone +441625 517920; e-mail jason.kettle@astrazeneca.com.

Present Address

†D.O.: The Paterson Institute for Cancer Research, University of Manchester, Wilmslow Road, Manchester M20 4BX, U.K.; e-mail dogilvie@picr.man.ac.uk.

Notes

The authors declare no competing financial interest.

ABBREVIATIONS USED

ATP, adenosine triphosphate; GSK3β, glycogen synthase kinase 3β; PDK1, 3-phosphoinositide-dependent protein kinase 1; mTOR, mammalian target of rapamycin; PH, pleckstrin homology; PI3K, phosphoinositide 3-kinase; SAR, structure−activity relationship

REFERENCES

(1) Liu, P.; Cheng, H.; Roberts, T. M.; Zhao, J. J. Targeting the phosphoinositide 3-kinase pathway in cancer. *Nat. Rev. Drug Discovery* **2009**, *8*, 627−644.

(2) Manning, B. D.; Cantley, L. C. Navigating downstream of AKT. *Cell* **2007**, *129*, 1261−1274.

(3) Bozulic, L.; Hemmings, B. A. PIKKing on PKB: Regulation of PKB activity by phosphorylation. *Curr. Opin. Cell Biol.* **2009**, *21*, 256−261.

(4) Sarbassov, D. D.; Guertin, D. A.; Ali, S. M.; Sabatini, D. M. Phosphorylation and regulation of Akt/PKB by the rictor-mTOR complex. *Science* **2005**, *307*, 1098−1101.

(5) Pearce, L. R.; Komander, D.; Alessi, D. R. The nuts and bolts of ABC protein kinases. *Nat. Rev. Mol. Cell Biol.* **2010**, *11*, 9−22.

(6) Mattmann, M. E.; Stoops, S. L.; Lindsley, C. W. Inhibition of Akt with small molecules and biologics: Historical perspective and current status of the patent landscape. *Expert Opin. Ther. Pat.* **2011**, *21* (9), 1309−1338.

(7) Hirai, H.; Sootome, H.; Nakatsuru, Y.; Miyama, K.; Taguchi, S.; Tsujioka, K.; Ueno, Y.; Hatch, H.; Majumder, P. K.; Pan, B.-S.; Kotani, H. MK-2206, an allosteric Akt inhibitor, enhances antitumor efficacy by standard chemotherapeutic agents or molecular targeted drugs in vitro and in vivo. *Mol. Cancer Ther.* **2010**, *9* (7), 1956−1967.

(8) Blake, J. F.; Xu, R.; Bencsik, J. R.; Xiao, D.; Kallan, N. C.; Schlachter, S.; Mitchell, I. S.; Spencer, K. L.; Banka, A. L.; Wallace, E. M.; Gloor, S. L.; Martinson, M.; Woessner, R. D.; Vigers, G. P. A.; Brandhuber, B. J.; Liang, J.; Safina, B. S.; Li, J.; Zhang, B.; Chabot, C.; Do, S.; Lee, L.; Oeh, J.; Sampath, D.; Lee, B. B.; Lin, K.; Liederer, B. M.; Skelton, N. J. Discovery and preclinical pharmacology of a selective ATP-competitive Akt inhibitor (GDC-0068) for the treatment of human tumors. *J. Med. Chem.* **2012**, *55*, 8110−8127.

(9) Pal, S. K.; Reckamp, K.; Yu, H.; Figlin, R. A. Akt inhibitors in clinical development for the treatment of cancer. *Expert Opin. Invest. Drugs* **2010**, *19* (11), 1355−1366.

(10) (a) McHardy, T.; Caldwell, J. J.; Cheung, K.-M.; Hunter, L. J.; Taylor, K.; Rowlands, M.; Ruddle, R.; Henley, A.; de Haven Brandon, A.; Valenti, M.; Davies, T. G.; Fazal, L.; Seavers, L.; Raynaud, F. I.; Eccles, S. A.; Aherne, G. W.; Garrett, M. D.; Collins, I. Discovery of 4-amino-1-(7H-pyrrolo[2,3-d]pyrimidin-4-yl)piperidine-4-carboxamides as selective, orally active inhibitors of protein kinase B (Akt). *J. Med. Chem.* **2010**, *53*, 2239−2249. (b) Caldwell, J. J.; Davies, T. G.; Donald, A.; McHardy, T.; Rowlands, M. G.; Aherne, G. W.; Hunter, L. K.;

Taylor, K.; Ruddle, R.; Raynaud, F. I.; Verdonk, M.; Workman, P.; Garrett, M. D.; Collins, I. Identification of 4-(4-aminopiperidin-1-yl)-7*H*-pyrrolo[2,3-*d*]pyrimidines as selective inhibitors of protein kinase B through fragment elaboration. *J. Med. Chem.* **2008**, *51*, 2147−2157.

(11) (a) Saxty, G.; Woodhead, S. J.; Berdini, V.; Davies, T. G.; Verdonk, M. L.; Wyatt, P. G.; Boyle, R. G.; Barford, D.; Downham, R.; Garrett, M. D.; Carr, R. A. Identification of inhibitors of protein kinase B using fragment-based lead discovery. *J. Med. Chem.* **2007**, *50*, 2293−2296. (b) Donald, A.; McHardy, T.; Rowlands, M. G.; Hunter, L. J. K.; Davies, T. G.; Berdini, V.; Boyle, R. G.; Aherne, G. W.; Garrett, M. D.; Collins, I. Rapid evolution of 6-phenylpurine inhibitors of protein kinase B through structure-based design. *J. Med. Chem.* **2007**, *50*, 2289−2292.

(12) (a) Ashton, K. S.; St. Jean, D. J., Jr.; Poon, S. F.; Lee, M. R.; Allen, J. G.; Zhang, S.; Lofgren, J. A.; Zhang, X.; Fotsch, C.; Hungate, R. Design and synthesis of novel amide AKT1 inhibitors with selectivity over CDK2. *Bioorg. Med. Chem. Lett.* **2011**, *21*, 5191−5196. (b) Bencsik, J. R.; Xiao, D.; Blake, J. F.; Kallan, N. C.; Mitchell, I. S.; Spencer, K. L.; Xu, R.; Gloor, S. L.; Martinson, M.; Risom, T.; Woessner, R. D.; Dizon, F.; Wu, W.-I.; Vigers, G. P. A.; Brandhuber, B. J.; Skelton, N. J.; Prior, W. W.; Murray, L. J. Discovery of dihydrothieno- and dihydrofuropyrimidines as potent pan Akt inhibitors. *Bioorg. Med. Chem. Lett.* **2010**, *20*, 7037−7041. (c) Free-man-Cook, K. D.; Autry, C.; Borzillo, G.; Gordon, D.; Barbacci-Tobin, E.; Bernardo, V.; Briere, D.; Clark, T.; Corbett, M.; Jakubczak, J.; Kakar, S.; Knauth, E.; Lippa, B.; Luzzio, M. J.; Mansour, M.; Martinelli, G.; Marx, M.; Nelson, K.; Pandit, J.; Rajamohan, F.; Robinson, S.; Subramanyam, C.; Wei, L.; Wythes, M.; Morris, J. Design of selective, ATP-competitive inhibitors of Akt. *J. Med. Chem.* **2010**, *53*, 4615−4622.

(13) Takahara, A.; Sugiyama, A.; Satoh, Y.; Yoneyama, M.; Hashimoto, K. Cardiovascular effects of Y-27632, a selective Rho-associated kinase inhibitor, assessed in the halothane-anesthetized canine model. *Eur. J. Pharmacol.* **2003**, *460*, 51−57.

(14) Davies, B. R.; Greenwood, H.; Dudley, P.; Crafter, C.; Yu, D.-H.; Zhang, J.; Li, J.; Gao, B.; Ji, Q.; Maynard, J.; Ricketts, S.-A.; Cross, D.; Cosulich, S.; Chresta, C. C.; Page, K.; Yates, J.; Lane, C.; Watson, R.; Luke, R.; Ogilvie, D.; Pass, M. Preclinical pharmacology of AZD5363, an inhibitor of AKT: Pharmacodynamics, antitumor activity, and correlation of monotherapy activity with genetic background. *Mol. Cancer Ther.* **2012**, *11*, 873−887.